1964

Compensation of a control system with saturation by means of a hysteresis element

Mansell Herbert Hopkins Jr.
Iowa State University

COMPENSATION OF A CONTROL SYSTEM WITH SATURATION BY MEANS OF A HYSTERESIS ELEMENT

by

Mansell Herbert Hopkins, Jr.

A Dissertation Submitted to the
Graduate Faculty in Partial Fulfillment of
The Requirements for the Degree of
DOCTOR OF PHILOSOPHY

Major Subject: Electrical Engineering

Approved:

Signature was redacted for privacy.

In Charge of Major Work

Signature was redacted for privacy.

Head of Major Department

Signature was redacted for privacy.

Dean of Graduate College

Iowa State University
Of Science and Technology
Ames, Iowa

1964

TABLE OF CONTENTS

I. INTRODUCTION

While there has been much literature published on the compensation of linear control systems, the subject of compensation of nonlinear systems has not been so comprehensively treated. This dissertation is an attempt to study comprehensively a particular type of nonlinear compensator for improving the performance of a position control system with saturation.

The phenomenon of saturation may be present inherently in a control system due to physical limitations of the devices used in the fixed plant, or it may be intentionally introduced by the designer in order to limit the magnitude of certain control system variables for safety or economy.

When saturation occurs in a control system the effect is usually a deterioration of system performance from the standpoint of speed of response. The overall effect is somewhat similar to a reduction in gain in a linear system. In the describing-function approach to the analysis of saturating amplifiers (1) the describing function (quasi-linear gain) of an amplifier with saturation has a value equal to the nominal gain of the amplifier for small sinusoidal inputs and drops off to a small value approaching zero for very large inputs.

The usual effect of a reduction in system gain in a linear control system is a slower response and thus a more stable, but sluggish, system. An exception to this is the conditionally stable system in which a reduction in gain can produce instability.

Hopkin (2) states that when the control system designer is confronted with the problem of saturation there are two alternatives: 1. to eliminate the source of saturation or 2. to design the system in such a way as

to minimize the effects of saturation and produce a satisfactory design in spite of the saturation.

If the latter of the two alternatives is chosen there are several different methods of compensation to be considered. Chen (3) used a quasi-linear approach to design a linear compensation network. This compensator was placed between the saturating element and the remainder of the control elements. Since it is impractical to design a series compensator for high power levels, it would seem that this method would not be suitable for compensation of a large-power element.

The approach of Hopkin (2) was to design a time optimal system and to modify this by using a narrow-proportional-band amplifier to control the manipulated variable and to give an improved response to a constant velocity input.

Chang and Archibald (4) designed a nonlinear compensator which stored energy in a capacitor during the saturation period. The amount of energy depended on the time integral of the excess error and was used to prolong the period of maximum signal to the power element and thus partially compensate for the loss of energy to the power element during the saturation period. The compensator was designed for systems in which linear phase-lead compensators produced saturation of amplifiers during rapid changes in input signals. The describing-function technique along with an analog computer study was used to analyze a type 2 system with saturation. It was observed that the compensation was not effective for systems with small damping ratios. No attempt was made to determine for what types of systems the compensator would be most effective or to design the compensator by other than trial and error methods.

The hysteresis element discussed in this dissertation utilizes the principle discussed by Chang and Archibald (4) combined with the concept of time optimality (5) to improve the step-input performance of a control system with saturation.

The hysteresis element will be defined as any nonlinear control element whose output at certain points is a double-valued function of its input. One of the most common types of hysteresis element is a magnetic relay which, due to hysteresis in the iron core, releases at a considerably lower current than is required for operation. The term negative hysteresis will be defined in the same manner as was done by Golden and Weaver (6) to be the type in which the output in the double-valued region takes on the larger of the two values when approached from above, i.e. the relay characteristic or the hysteresis curve for ferromagnetic materials. The linear, phase-lead network is analogous to a positive-hysteresis element while the phase-lag network is analogous to a negative-hysteresis element. In fact, if one is careful not to carry the analogy too far, some insight can be gained by comparing nonlinear hysteresis elements with phase-lead or phase-lag networks.

Since the effect of saturation in a control system is to reduce the apparent low-frequency gain of the system, the compensator should have a tendency to increase the low-frequency gain in order to improve the performance of a system with saturation. This is precisely the effect of a phase-lag network and would lead one to conclude that the negative-hysteresis characteristic possibly might be effective in improving the performance of such a system.

It is important to note that while in saturation a control system is

essentially operating open-loop and any series compensator placed in front of the saturating element has a limited time within which to perform its function. That is to say that the compensator must modify the system response either before saturation occurs or after the system drops out of saturation. The negative-hysteresis element modifies the system by holding it into saturation for a period longer than normal. If, in the uncompensated system, the period after dropout is relatively long compared to the duration of saturation, the hysteresis compensator may have a marked influence on the system response, otherwise it probably will prove ineffective as a compensator. In this respect the nonlinear-hysteresis element differs from a linear system whose form of response is unaffected by the magnitude of its inputs.

The purpose of this dissertation is to study the hysteresis element used as compensation for saturation with the following goals in mind:

1. To arrive at a procedure for the design of hysteresis compensation which eliminates as much trial and error as possible.
2. To determine the type of systems for which hysteresis can be effective.
3. To verify the results of 1 and 2 by means of an analog-computer study.

II. COMPENSATION FOR SATURATION USING HYSTERESIS ELEMENTS

A. Analytical Considerations

The control system shown in Figure 1 is a typical second-order, position-control system consisting of an error-sensing device, a power amplifier, and an armature-controlled, direct-current motor. The power amplifier is assumed to have the hard-saturation type of input-output characteristic. This particular form of nonlinearity was chosen because it is sectionally linear, thus facilitating analytical calculation of the system response, and because it can be simulated with ease on an analog computer. It has been found in practice that the simulation of actual nonlinearities by sectionally linear curves can give satisfactorily accurate results for most problems.

The closed-loop transfer function of the system when operating in the linear region is given by the following equation.

$$\frac{C(s)}{R(s)} = \frac{\omega_o^2}{s^2 + 2 \zeta \omega_o s + \omega_o^2} \qquad (1)$$

When the system error is large enough that the power amplifier is saturated, the system is operating open-loop with a constant input voltage to the motor equal to the saturation level of the power amplifier. The relationship between the Laplace transforms of the motor input and output is given by the following equation.

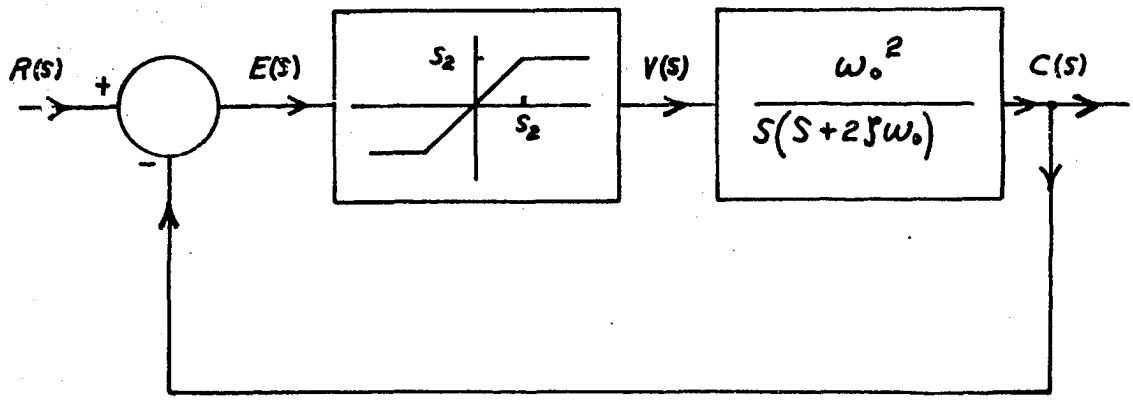

Figure 1. Position control system with saturating amplifier

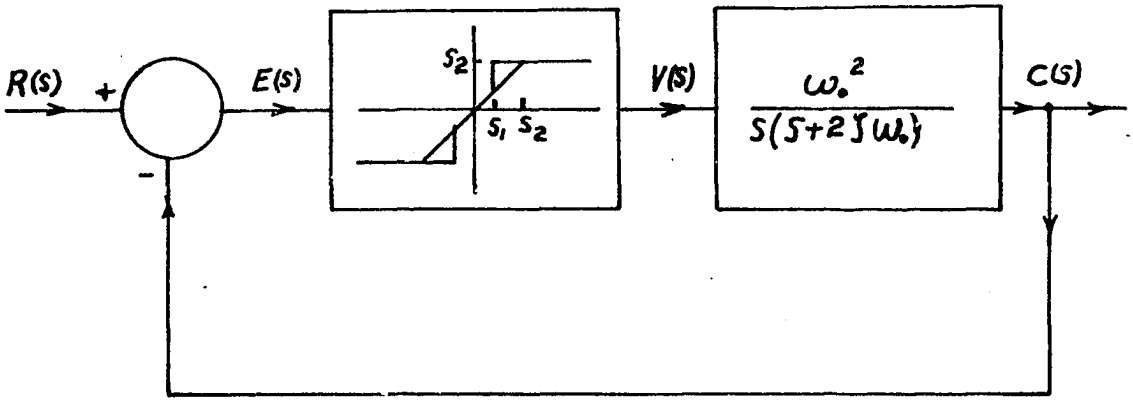

Figure 2. Position control system with saturating amplifier and hysteresis compensator

$$\frac{C(s)}{V(s)} = \frac{\omega_o^2}{s(s + 2\zeta\omega_o)} \qquad (2)$$

Since the system is sectionally linear, its error response to an initial disturbance of the output variable larger than the saturation level of the amplifier can be calculated analytically by using two different sets of linear differential equations to describe the response of the system during the saturated period and during the linear period. During the saturation period the error response is described by the following equation.

$$\ddot{e} + 2\zeta\omega_o \dot{e} = \pm S_2 \qquad (3)$$

Here the dot notation is used to indicate the derivative with respect to time.

After the system error is reduced below the saturation level, the error response is described by the equation,

$$\ddot{e} + 2\zeta\omega_o \dot{e} + \omega_o^2 e = 0 \qquad (4)$$

The calculation of the error response of the compensated system is identical to that of the uncompensated system with the exception that the duration of saturation is prolonged by the compensator. A block diagram of the compensated system is shown in Figure 2. The emphasis on error response is a matter of convenience. It can be shown that the response of

the system to a step input has the same form as the error response of the autonomous system subjected to an initial position disturbance.

If the compensator is to improve the speed of response of the system, the improvement would have to be accomplished at the expense of increasing the overshoot in all except the extremely overdamped case. This means that the dropout point should be chosen so as to obtain the fastest response possible without exceeding the maximum allowable overshoot.

Although the previously outlined method can readily be used for the analysis of the system once the dropout point has been chosen it does not lend itself readily to aiding in determining where the dropout point should be. A better approach to the problem from the standpoint of designing the compensator is the use of a phase-plane plot. This method requires the construction of two phase-plane trajectories, one for the second-order, autonomous, linear system with no saturating element where the initial condition is a displacement from the equilibrium position, and another for the open-loop system subjected to a constant voltage input equal to the saturation voltage and starting from rest at the initial displacement. Both trajectories are time-scaled either by graphical means or by calculation of the time response. The graphical method, if carefully done, seems to give sufficiently accurate results with much less work.

To illustrate the use of the phase-plane technique in the design of a nonlinear compensator, a problem will be worked for the system of Figures 1 and 2 with a damping ratio, ζ, of 0.8 and a saturation level of 0.5 units.

The normalized differential equation for the linear system is

$$\ddot{e} + 2\zeta\dot{e} + e = 0 \qquad (5)$$

and that for the system while in saturation is

$$\ddot{e} + 2\zeta\dot{e} = +0.5 \qquad (6)$$

It will be assumed that the system is subjected to a maximum initial displacement of 1.0 units, which is considerably above the saturation level of the power amplifier. It will also be assumed that it is desired to analyze the response for smaller initial displacements and to have a maximum overshoot of approximately 0.05 units.

1. Construction of phase-plane trajectories

The first step is the plotting and time-scaling of trajectory 1 in Figure 3 which is the trajectory of the motor and load with a constant voltage of -0.5 units starting from the initial point of e = -1.0. The next step is to plot and time-scale a trajectory for the linear system. This trajectory extends from the initial point at e = -1.0 to the first overshoot and is called trajectory 3 in Figure 3.

It should be pointed out here that trajectory 3 contains the information needed for plotting all other trajectories for the unsaturated system since the linear trajectory for a smaller initial displacement is merely a scaled-down version of trajectory 3. Both trajectories were plotted using Pell's method (7). The response for the uncompensated system can be obtained

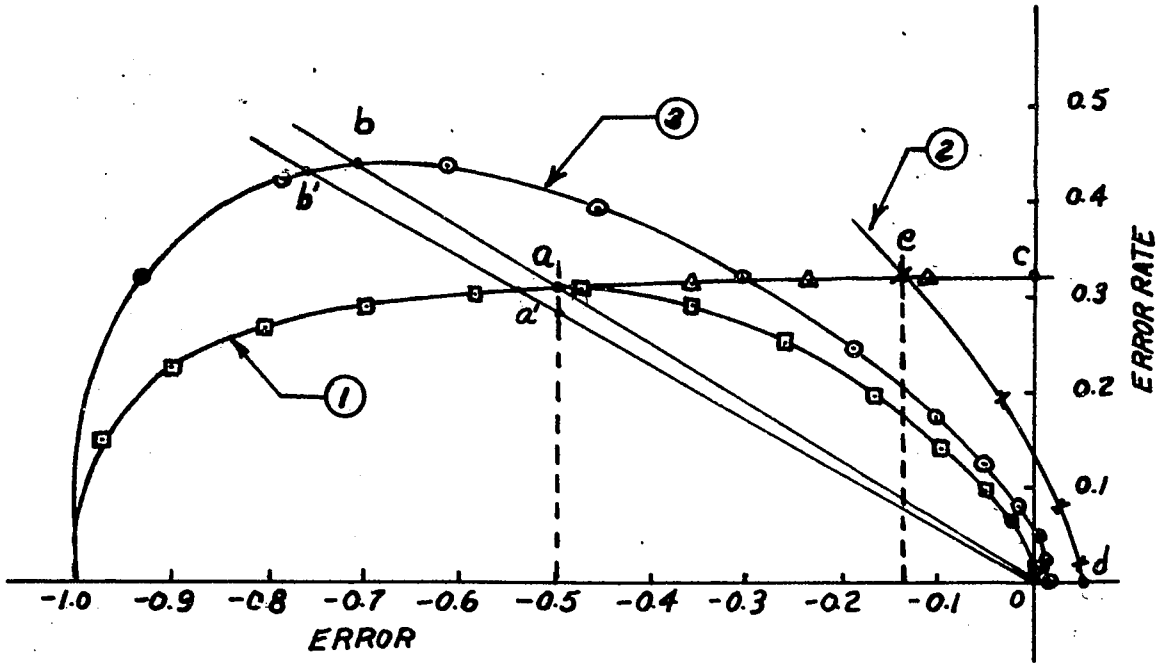

Figure 3. Time-scaled trajectories used to design hysteresis compensator (timing marks spaced 0.4 time units apart) (1) saturated trajectory, (2) after-dropout trajectory, and (3) linear trajectory

by following trajectory 1 until the error is reduced to the saturation level of the amplifier and then following a linear trajectory for the remainder of the response. Point a on Figure 3 is the point where the uncompensated system drops out of saturation. It is found to be approximately 3.8 time units on a normalized time scale from the first overshoot. This is determined by drawing a line from the origin through point a intersecting trajectory 3 at point b and then counting the time units from point b to the first overshoot. The points on Figure 3 are plotted with 0.4 time units between adjacent points. An alternate method is to complete the uncompensated trajectory from point a to the origin and then place a time scale directly on it. This was done on Figure 3 in order that the time response could be read directly from the phase-plane plot. This, however, is not necessary since trajectories 1 and 3 contain all the information that is required for obtaining the time response of the saturated system for any initial position and any dropout point. For example, with an initial error of -0.8 units the time response while the system is saturated can be obtained by reading time values from trajectory 1 and subtracting 2 units from the error magnitude at that point. From Figure 3 it can be seen that the dropout point would occur at a point with coordinates (-0.5, 0.285) which corresponds to 1.6 time units on trajectory 1. If the line Oa'b' is drawn through the new dropout point it will be seen to intersect trajectory 3 at a point corresponding to T = 0.85 on trajectory 3. The remainder of the time response can be determined by the following steps:

1. Determining the scale factor relating the linear portion of the new trajectory with trajectory 3. In this case it is the ratio Oa'/Ob' which is approximately 0.659.

2. Relate the time-scale on trajectory 3 to the new trajectory by noting that the point T = 0.85 on trajectory 3 corresponds to 1.6 seconds on the new trajectory, i.e. $T_{new} = T + 0.75$.
3. Compute values for time and position for the remainder of the response by taking points on trajectory 3, multiplying the magnitude by the ratio Oa'/Ob' and adding 0.75 seconds to the time taken from the linear trajectory.

Although the above procedure may seem to be an indirect method of obtaining the time response, it does have the advantage that it is necessary to plot and time-scale only one set of phase-plane trajectories to calculate the time response for a number of different sets of initial conditions.

2. Design of the nonlinear compensator

An attempt will be made to improve the response time of the system for step inputs through the use of a nonlinear hysteresis element whose function is to hold the system in saturation for a period longer than normal. The compensator makes it possible to obtain the maximum control effort from the motor for a longer period of time than would be possible with the uncompensated system. The above point is illustrated by Figure 4 which shows the input signal to the motor for the response of a second-order system with an initial error of 1.0 units and a damping ratio of 0.8. Curves a, b, and c of Figure 4 show the motor input for the uncompensated, compensated, and linear systems respectively.

An inspection of Figure 3 will show that the dropout point can be chosen anywhere between points a and c on trajectory 1. Since all points on trajectory ac represent higher velocities than do corresponding points on trajectory aO, it follows that the system will reach zero error most

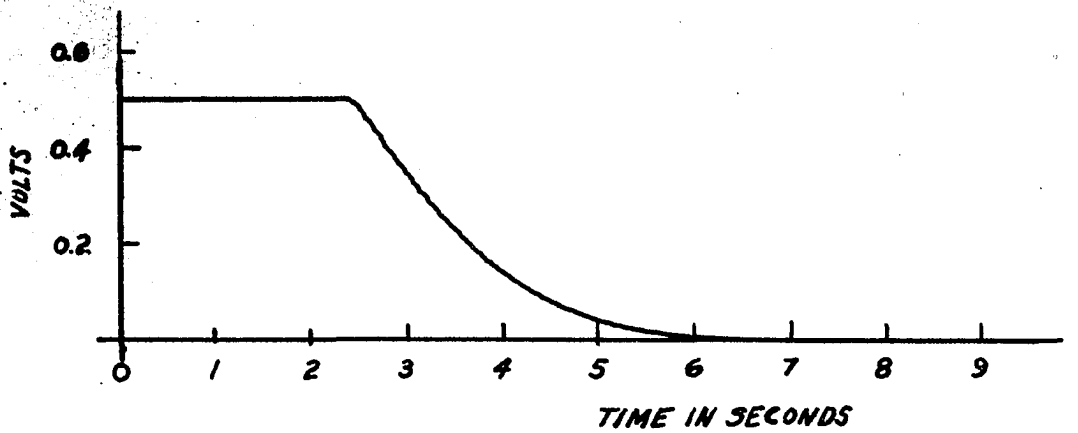

Figure 4a. Motor input versus time for uncompensated system of Figure 1 with damping ratio of 0.8 and an initial error of 1.0 units

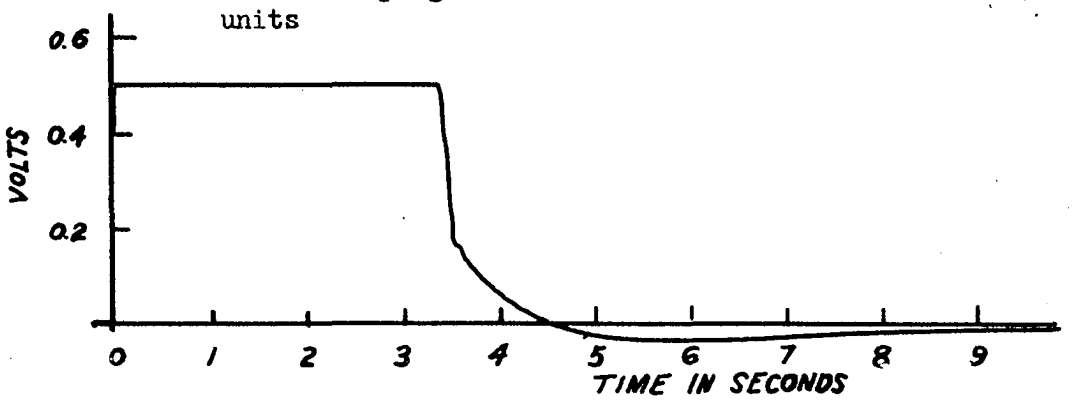

Figure 4b. Motor input versus time for hysteresis compensated system of Figure 2 with damping ratio of 0.8 and an initial error of 1.0 units.

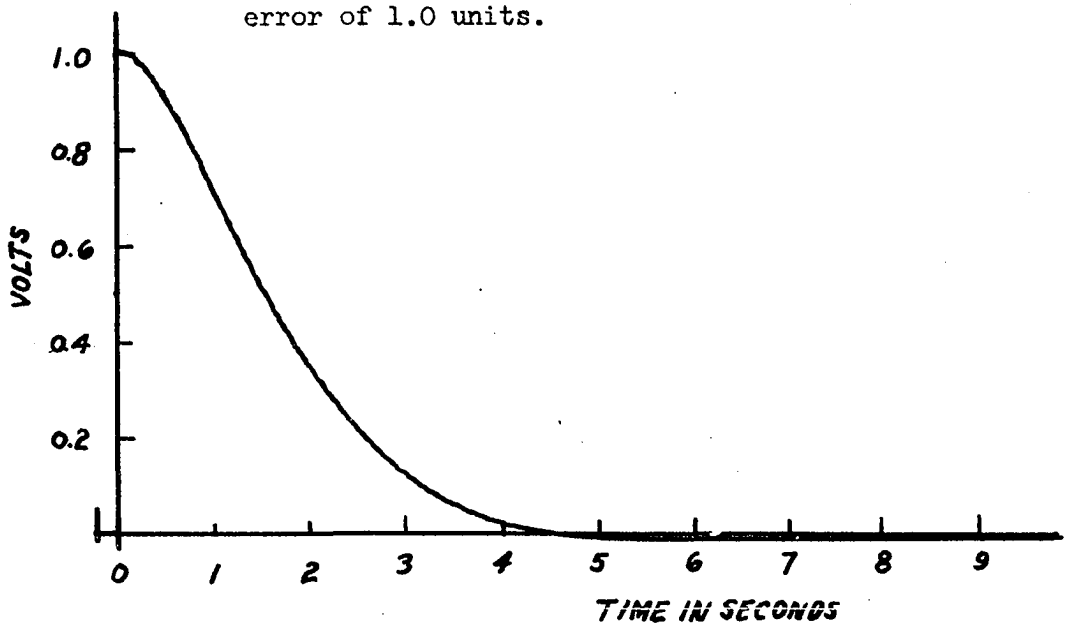

Figure 4c. Motor input versus time for system without saturation with damping ratio of 0.8 and an initial error of 1.0 units

rapidly if it remains saturated until the error is reduced to zero. If it is desired that the system reach zero error in the minimum possible time with no consideration given to overshoot, point c should be chosen as the dropout point. If, however, a limit is to be placed on overshoot, the dropout point will be chosen somewhere between points a and c on trajectory 1. In this example the dropout point will be chosen so as to limit the overshoot to approximately 0.05 units. The dropout point can be determined by constructing a third trajectory for the linear system (see Figure 3) starting from point d which corresponds to an overshoot of 0.05 units and extending the trajectory backwards to point e where it intersects trajectory 1. This new trajectory will be called trajectory 2. The value of the error at point e is the dropout point that will give the fastest possible response to a step input without exceeding the overshoot limit. From Figure 3 it can be seen that the error at the dropout point is 0.14 units.

The trajectory of the compensated system will follow trajectory 1 from the initial point to the dropout point and then will follow trajectory 2 to the origin.

3. Calculated results

The results of the calculations are tabulated in Tables 1 through 3 for the second-order system with a damping ratio of 0.8. These calculated points will be later superimposed on the experimental time response curves of Figures 9 through 11.

Data from similar calculations made with damping ratios of 1.0 and 0.5 are shown in Tables 4 through 6 and Tables 7 through 9 respectively.

Table 1. Calculated time response of system with damping ratio 0.8, initial error of 1.0 and dropout point of 0.14

1 Uncompensated		2 Compensated		3 Linear	
T	$\frac{e}{e_o}$	T	$\frac{e}{e_o}$	T	$\frac{e}{e_o}$
0	1.00	0	1.00	0	1.00
0.4	0.97	0.4	0.97	0.4	0.93
0.8	0.90	0.8	0.90	0.8	0.78
1.2	0.80	1.2	0.80	1.2	0.61
1.6	0.69	1.6	0.69	1.6	0.46
2.0	0.58	2.0	0.58	2.0	0.30
2.4	0.46	2.4	0.46	2.4	0.19
2.8	0.36	2.8	0.36	2.8	0.11
3.2	0.26	3.2	0.26	3.2	0.06
3.6	0.17	3.5	0.14	3.6	0.02
4.0	0.11	3.9	0.03	4.0	0
4.4	0.06	4.11	0	4.6	-0.02
4.8	0.03	4.5	-0.04		
5.2	0.01	5.1	-0.04		

Table 2. Calculated time response of system with damping ratio of 0.8, initial error of 0.8 and dropout point of 0.14

1 Uncompensated		2 Compensated		3 Linear	
T	$\frac{e}{e_o}$	T	$\frac{e}{e_o}$	T	$\frac{e}{e_o}$
0	1.00	0	1.00	0	1.00
0.4	0.96	0.4	0.96	0.4	0.93
0.8	0.87	0.8	0.87	0.8	0.78
1.2	0.75	1.2	0.75	1.2	0.61
1.6	0.62	1.6	0.62	1.6	0.46
1.75	0.57	2.0	0.48	2.0	0.30
2.35	0.38	2.4	0.34	2.4	0.19
2.75	0.25	2.86	0.18	2.8	0.11
3.15	0.16	3.06	0.10	3.2	0.06
3.55	0.09	3.46	0	3.6	0.02
3.95	0.05	3.86	-0.05	4.0	0
4.35	0.02	4.21	-0.06	4.6	-0.02
4.75	0				

Table 3. Calculated time response of system with damping ratio of 0.8, initial error of 0.6 and dropout point of 0.14

1 Uncompensated		2 Compensated		3 Linear	
T	$\frac{e}{e_o}$	T	$\frac{e}{e_o}$	T	$\frac{e}{e_o}$
0	1.00	0	1.0	0	1.00
0.4	0.95	0.4	0.95	0.4	0.93
0.8	0.83	0.8	0.84	0.8	0.78
1.2	0.67	1.2	0.67	1.2	0.61
1.6	0.51	1.6	0.48	1.6	0.46
2.0	0.36	2.0	0.30	2.0	0.30
2.4	0.24	2.2	0.22	2.4	0.19
2.8	0.14	2.4	0.133	2.8	0.11
3.2	0.08	2.8	0.02	3.2	0.06
3.6	0.04	3.2	-0.03	3.6	0.02
4.2	0	3.6	-0.07	4.0	0
4.8	-0.01	3.9	-0.07	4.6	-0.02

Table 4. Calculated time response of system with damping ratio of 1.0, initial error of 1.0 and dropout point of 0.055

1 Uncompensated		2 Compensated		3 Linear	
T	$\frac{e}{e_o}$	T	$\frac{e}{e_o}$	T	$\frac{e}{e_o}$
0	1.00	0	1.00	0	1.00
0.4	0.96	0.4	0.96	0.4	0.94
0.8	0.89	0.8	0.89	0.8	0.81
1.2	0.81	1.2	0.81	1.2	0.66
1.6	0.72	1.6	0.72	1.6	0.52
2.0	0.63	2.0	0.63	2.0	0.40
2.4	0.54	2.4	0.54	2.4	0.30
2.8	0.44	2.8	0.44	2.8	0.23
3.2	0.36	3.2	0.34	3.2	0.17
3.6	0.28	3.6	0.24	3.6	0.13
4.0	0.22	4.0	0.14	4.0	0.09
4.4	0.17	4.34	0.05	5.0	0.04
4.8	0,13	4.54	0.01	6.0	0.005
5.2	0.09	4.74	-0.01		
5.6	0.07	4.94	-0.03		
6.0	0.05	5.14	-0.04		
6.4	0.03	5.54	-0.05		
6.8	0.015				

Table 5. Calculated time response of system with damping ratio of 1.0, initial error of 0.8 and dropout point of 0.055

1 Uncompensated		2 Compensated		3 Linear	
T	$\frac{e}{e_o}$	T	$\frac{e}{e_o}$	T	$\frac{e}{e_o}$
0	1.00	0	1.00	0	1.00
0.4	0.95	0.4	0.95	0.4	0.94
0.8	0.86	0.8	0.86	0.8	0.81
1.2	0.76	1.2	0.76	1.2	0.66
1.6	0.65	1.6	0.65	1.6	0.52
2.0	0.55	2.0	0.54	2.0	0.40
2.4	0.45	2.4	0.43	2.4	0.30
2.8	0.35	2.8	0.30	2.8	0.23
3.2	0.29	3.2	0.18	3.2	0.17
3.6	0.21	3.54	0.06	3.6	0.13
4.0	0.16	3.74	0.013	4.0	0.09
4.4	0.11	3.94	-0.013	5.0	0.04
4.8	0.09	4.14	-0.04	6.0	0.005
5.2	0.06	4.34	-0.05		
		4.54	-0.06		
		4.74	-0.06		

Table 6. Calculated time response of system with damping ratio of 1.0, initial error of 0.6 and dropout point of 0.055

1 Uncompensated		2 Compensated		3 Linear	
T	$\frac{e}{e_o}$	T	$\frac{e}{e_o}$	T	$\frac{e}{e_o}$
0	1.00	0	1.00	0	1.00
0.4	0.92	0.4	0.94	0.4	0.94
0.8	0.82	0.8	0.82	0.8	0.81
0.95	0.79	1.2	0.68	1.2	0.66
1.35	0.64	1.6	0.53	2.0	0.40
1.75	0.51	2.0	0.38	2.4	0.30
2.15	0.39	2.4	0.23	2.8	0.23
2.55	0.29	2.8	0.07	3.2	0.17
2.95	0.22	3.0	0.02	3.6	0.13
3.35	0.165	3.2	-0.03	4.0	0.09
3.75	0.126	3.4	-0.05	5.0	0.04
4.15	0.087	3.6	-0.07	6.0	0.005
5.15	0.039	3.8	-0.08		
6.15	0.049	4.0	-0.08		

Table 7. Calculated time response of system with damping ratio of 0.5, initial error of 1.0 and dropout point of 0.215

1 Uncompensated		2 Compensated		3 Linear	
T	$\frac{e}{e_o}$	T	$\frac{e}{e_o}$	T	$\frac{e}{e_o}$
0	1.00	0	1.00	0	1.00
0.4	0.96	0.4	0.96	0.4	0.92
0.8	0.88	0.8	0.88	0.8	0.74
1.2	0.73	1.2	0.73	1.2	0.67
1.6	0.58	1.6	0.58	1.6	0.32
1.8	0.50	1.8	0.50	2.0	0.11
2.0	0.42	2.0	0.41	2.4	-0.03
2.4	0.25	2.4	0.21	2.8	-0.12
2.8	0.09	2.8	0.04	3.2	-0.17
3.2	0.024	3.2	-0.08	3.6	-0.16
3.6	0.094	3.6	-0.15	4.0	-0.14
4.0	0.133	4.0	-0.17		
4.4	0.126	4.6	-0.14		

Table 8. Calculated time response of system with damping ratio of 0.5, initial error of 0.8 and dropout point of 0.215

1 Uncompensated		2 Compensated		3 Linear	
T	$\frac{e}{e_o}$	T	$\frac{e}{e_o}$	T	$\frac{e}{e_o}$
0	1.00	0	1.00	0	1.00
0.4	0.95	0.4	0.95	0.4	0.92
0.8	0.85	0.8	0.85	0.8	0.74
1.2	0.66	1.2	0.66	1.2	0.67
1.3	0.62	1.4	0.58	1.6	0.32
1.8	0.39	2.0	0.23	2.0	0.11
2.2	0.18	2.2	0.14	2.4	-0.03
2.6	0.03	2.6	-0.04	2.8	-0.12
3.0	-0.07	3.0	-0.15	3.2	-0.16
3.4	-0.14	3.4	-0.21	4.0	-0.14
3.8	-0.16	3.8	-0.20		
4.2	-0.14	4.2	-0.18		

Table 9. Calculated time response of system with damping ratio of 0.5, initial error of 0.6 and dropout point of 0.215

1 Uncompensated		2 Compensated		3 Linear	
T	$\frac{e}{e_o}$	T	$\frac{e}{e_o}$	T	$\frac{e}{e_o}$
0	1.00	0	1.00	0	1.00
0.4	0.95	0.4	0.92	0.4	0.92
0.7	0.85	0.8	0.80	0.8	0.74
0.9	0.74	1.2	0.33	1.2	0.67
1.3	0.665	1.5	0.36	1.6	0.32
1.7	0.318	1.9	0.15	2.0	0.11
2.1	0.11	2.3	-0.04	2.4	-0.03
2.5	-0.03	2.7	-0.165	2.8	-0.12
2.9	-0.12	3.1	-0.23	3.2	-0.16
3.3	-0.17	3.5	-0.22	4.0	-0.14
3.7	-0.16	3.9	-0.19		
4.1	-0.14	4.9	-0.07		
5.1	-0.05				

B. Analog Computer Study

1. Simulation of the nonlinear system

As verification of the calculations the systems shown in Figure 1 and Figure 2 were simulated on an analog computer and recordings were made of both the time response and the phase-plane trajectories of the compensated and uncompensated systems.

Figure 5 shows the analog computer circuit used to simulate the hysteresis compensator and saturating amplifier while Figures 6a, 6b, and 6c show the input-output characteristic of the hysteresis compensator, the saturating amplifier, and the combined characteristic. The analog computer circuit for simulating the entire system is shown in Figure 7.

The timing pulses for obtaining time-scaled, phase-plane trajectories were provided by the circuit of Figure 8. These timing pulses were fed into the y-axis of the x-y plotter along with the error-velocity signal. The timing circuit differentiates a square wave generated by a low-frequency signal generator. The pulses thus obtained operate an auxiliary relay which locks up through a holding circuit and starts the problem on the computer by closing a circuit to the operate relay on the analog computer. The effect of the residual magnetism of the relay makes it possible to cause the relay to operate on pulses of one polarity only. The limiter shown on amplifier 11 of Figure 8 is set to eliminate either all positive or all negative pulses, depending on which pulses are not wanted, and to limit the amplitude of the desired pulses. If the computer time is made slow enough relative to the pulse duration, the pulses produce convenient timing marks on the phase-plane trajectories. The trajectories obtained

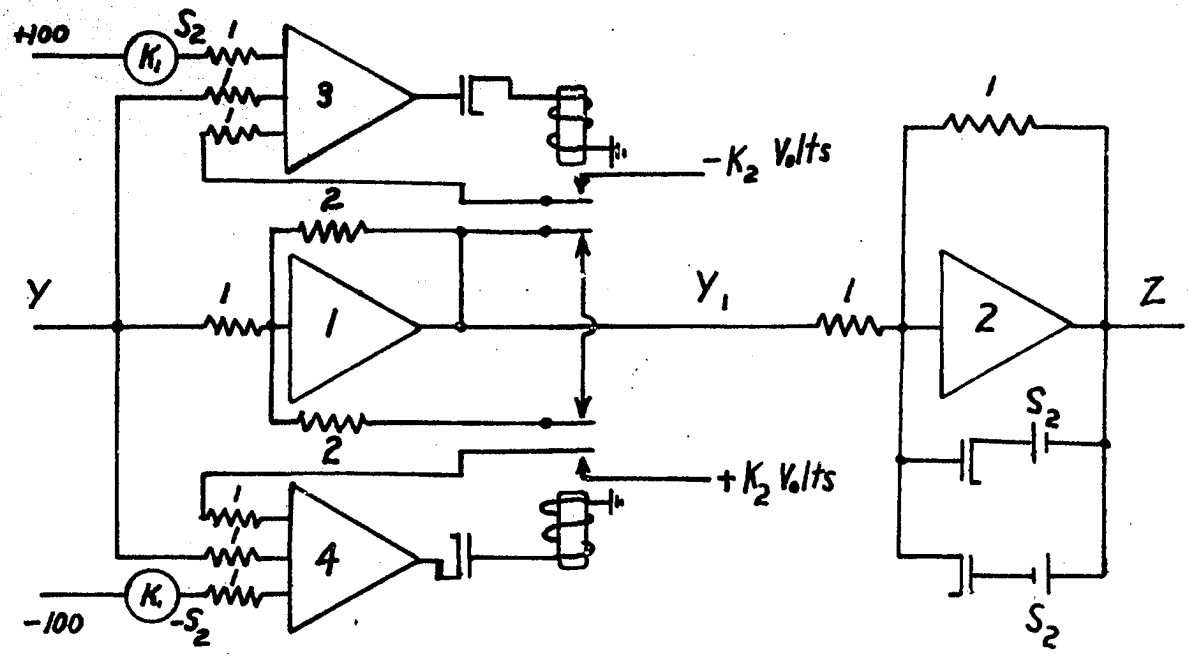

Figure 5. Analog computer simulation of hysteresis compensator and limiter

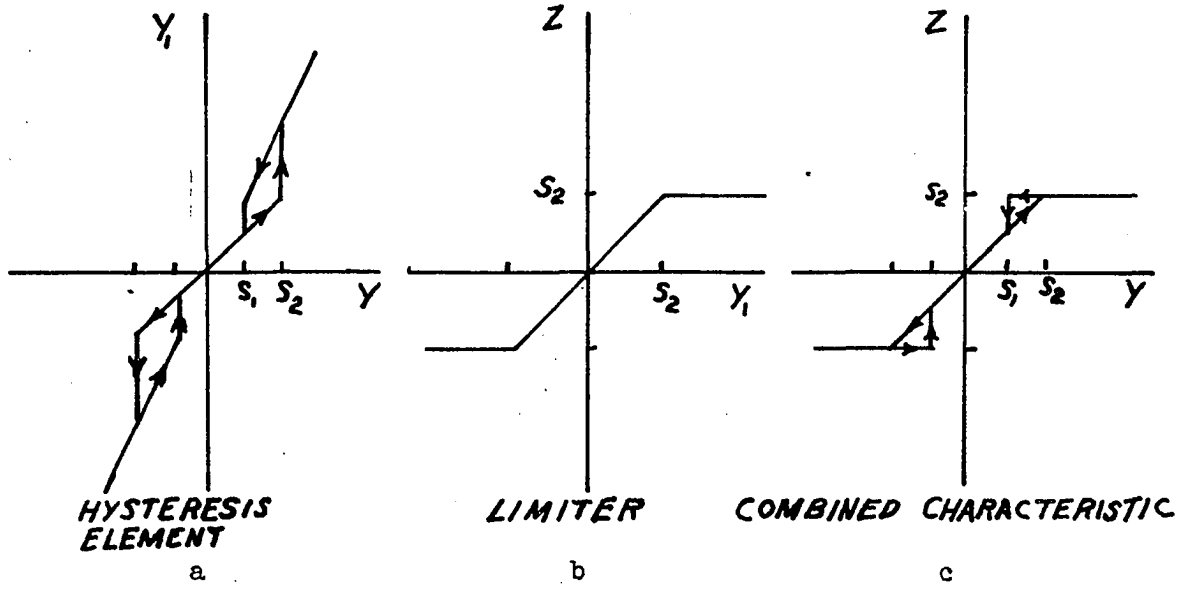

Figure 6. Input-output characteristics

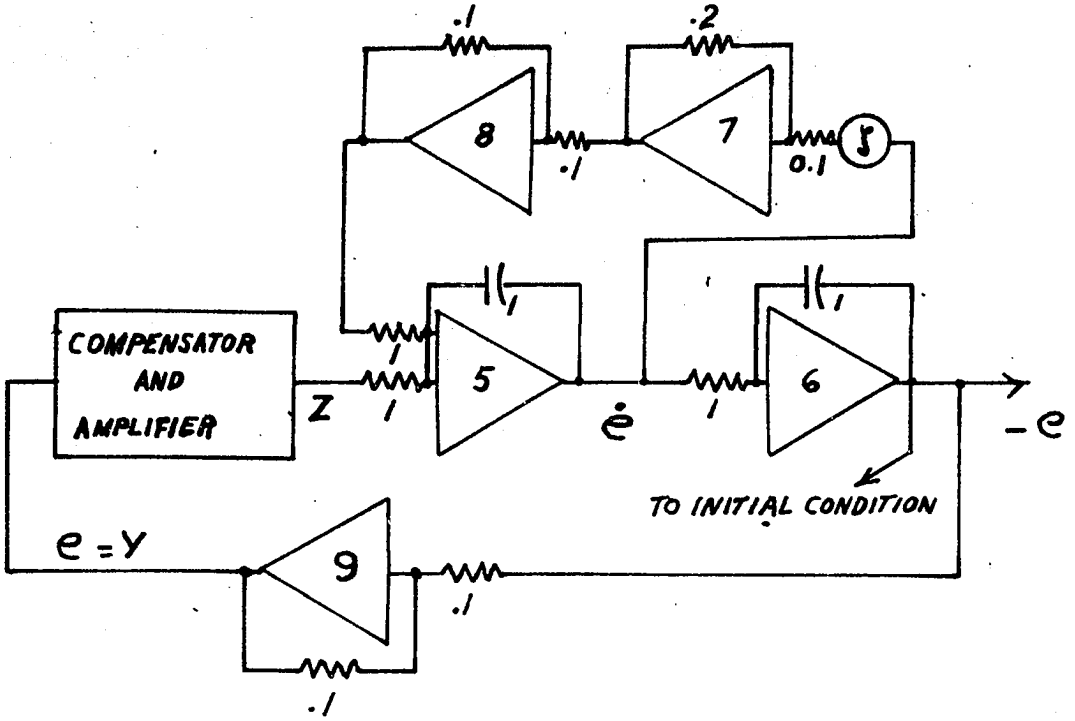

Figure 7. Analog simulation of nonlinear system

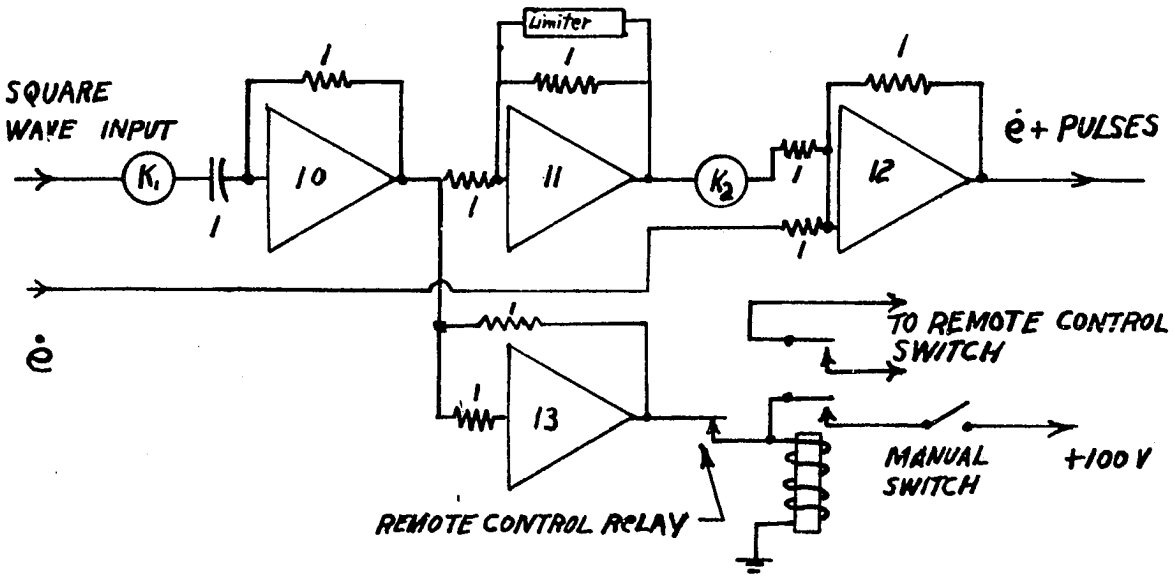

Figure 8. Analog computer connections for obtaining timing pulses

in this manner are shown in Figures 18 through 26.

2. Results of the computer study

Recordings of the time responses for each of the systems studied previously are shown in Figures 9 through 17. For comparison the calculated results are superimposed on the recorded curves. Tabulated values of delay time, rise time, settling time, amount of overshoot, and percentage overshoot are given in Tables 10 through 12. The following definitions are used for the first three quantities mentioned above:

1. The delay-time, T_d, is defined as the time required for the step response to reach 50 percent of its total change.
2. The rise time, T_r, is defined as the time for the system response to go from 10 percent to 90 percent of its total change.
3. The settling time, T_s, is defined as the shortest time required for the system error to be reduced to a magnitude of 0.05 units. (This is not the usual definition of settling time but it is more meaningful in this case).

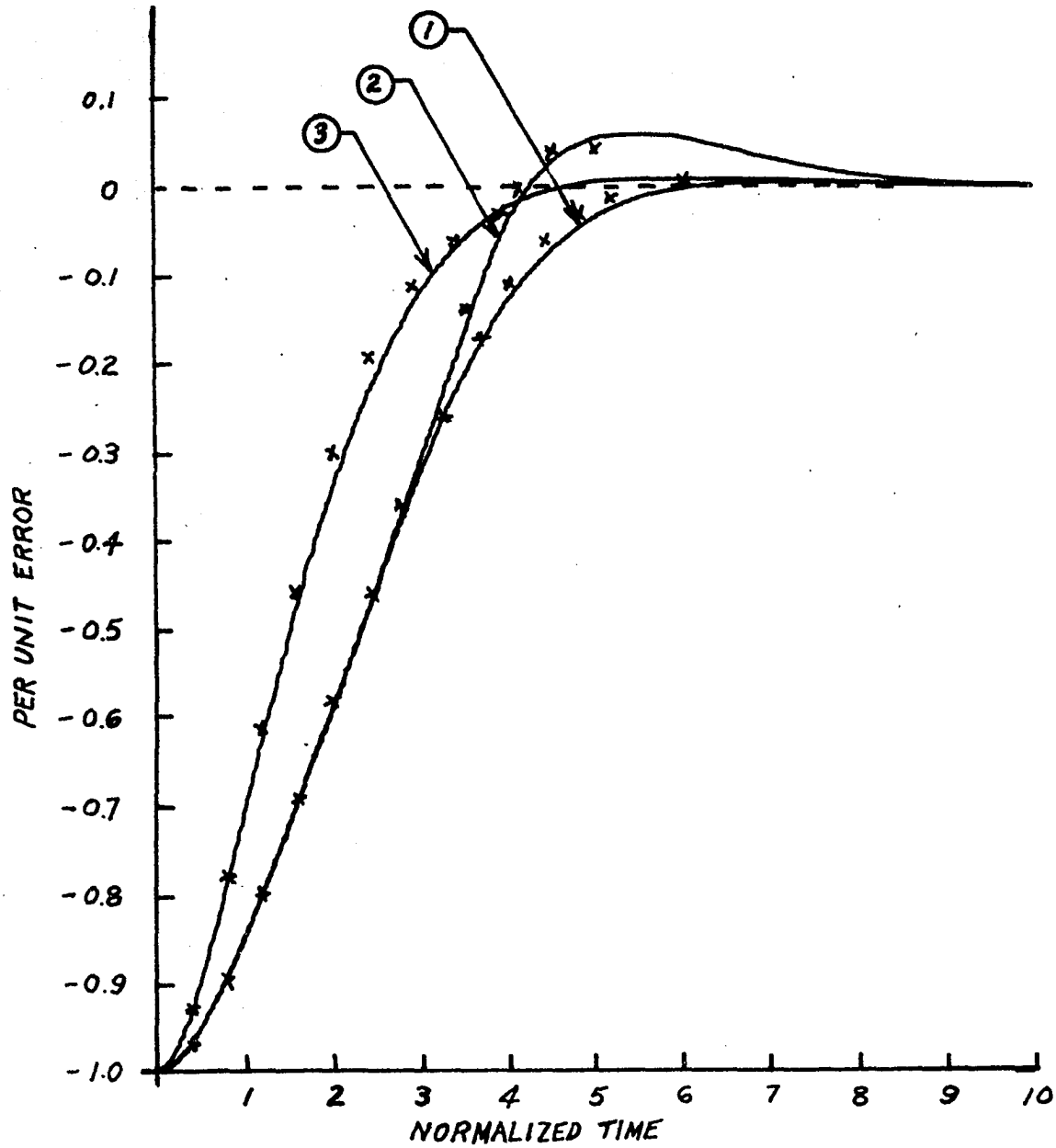

Figure 9. (1) Uncompensated, (2) compensated, and (3) linear error response recordings with superimposed calculated points for a system with damping ratio of 0.8 and initial error of 1.0

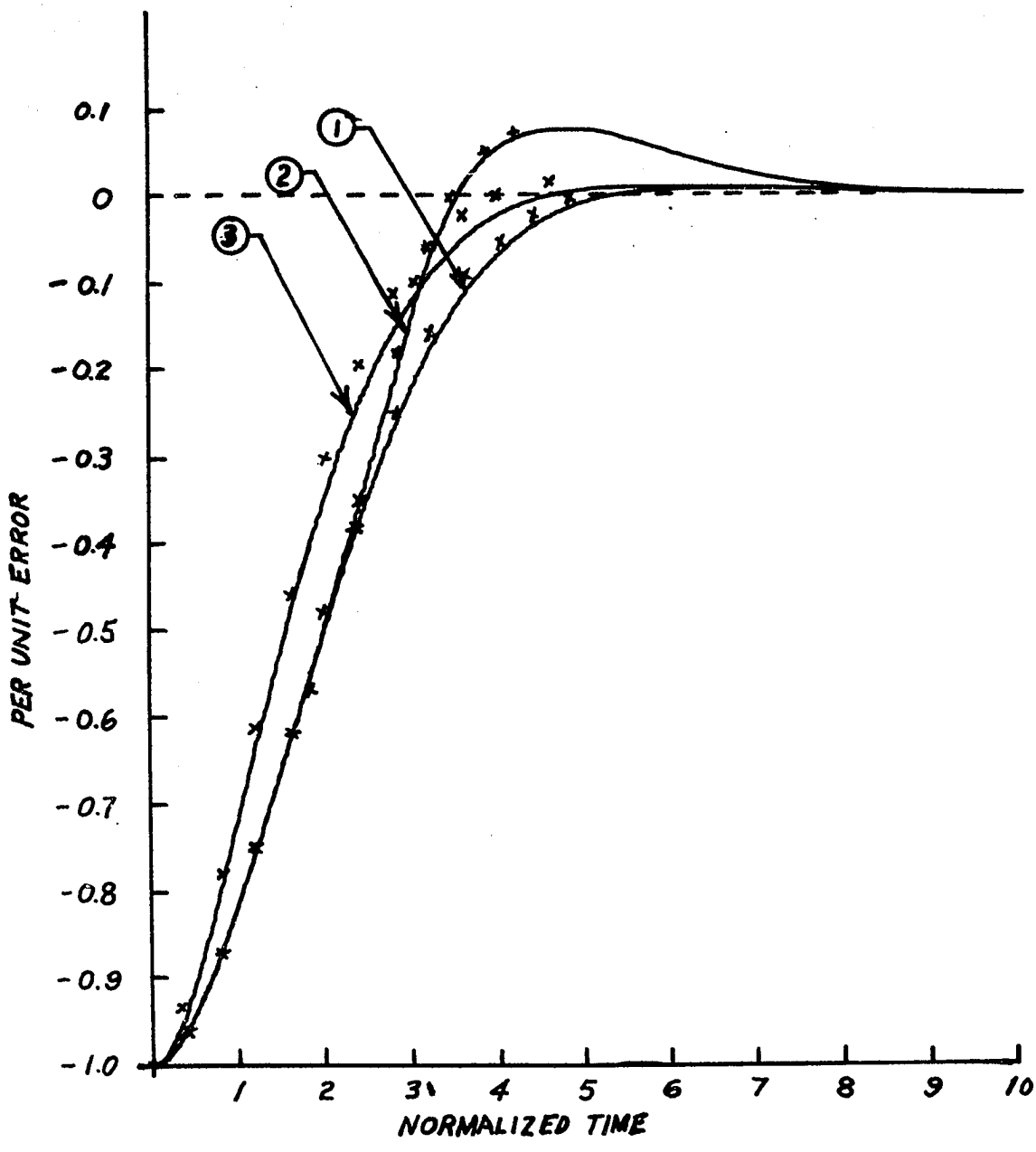

Figure 10. (1) Uncompensated, (2) compensated, and (3) linear error response recordings with superimposed calculated points for a system with damping ratio of 0.8 and initial error of 0.8

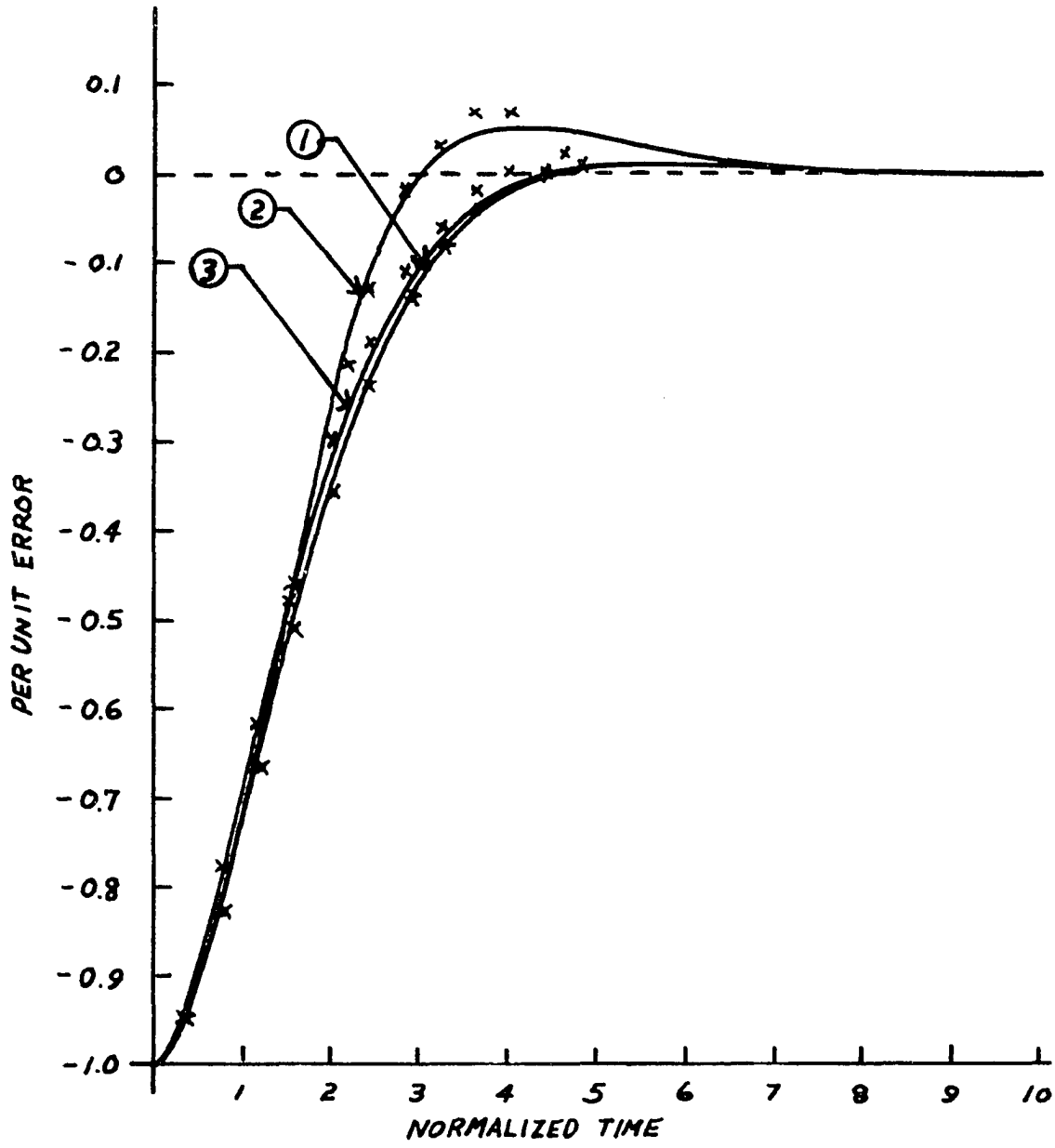

Figure 11. (1) Uncompensated, (2) compensated, and (3) linear error response recordings with superimposed calculated points for a system with damping ratio of 0.8 and initial error of 0.6

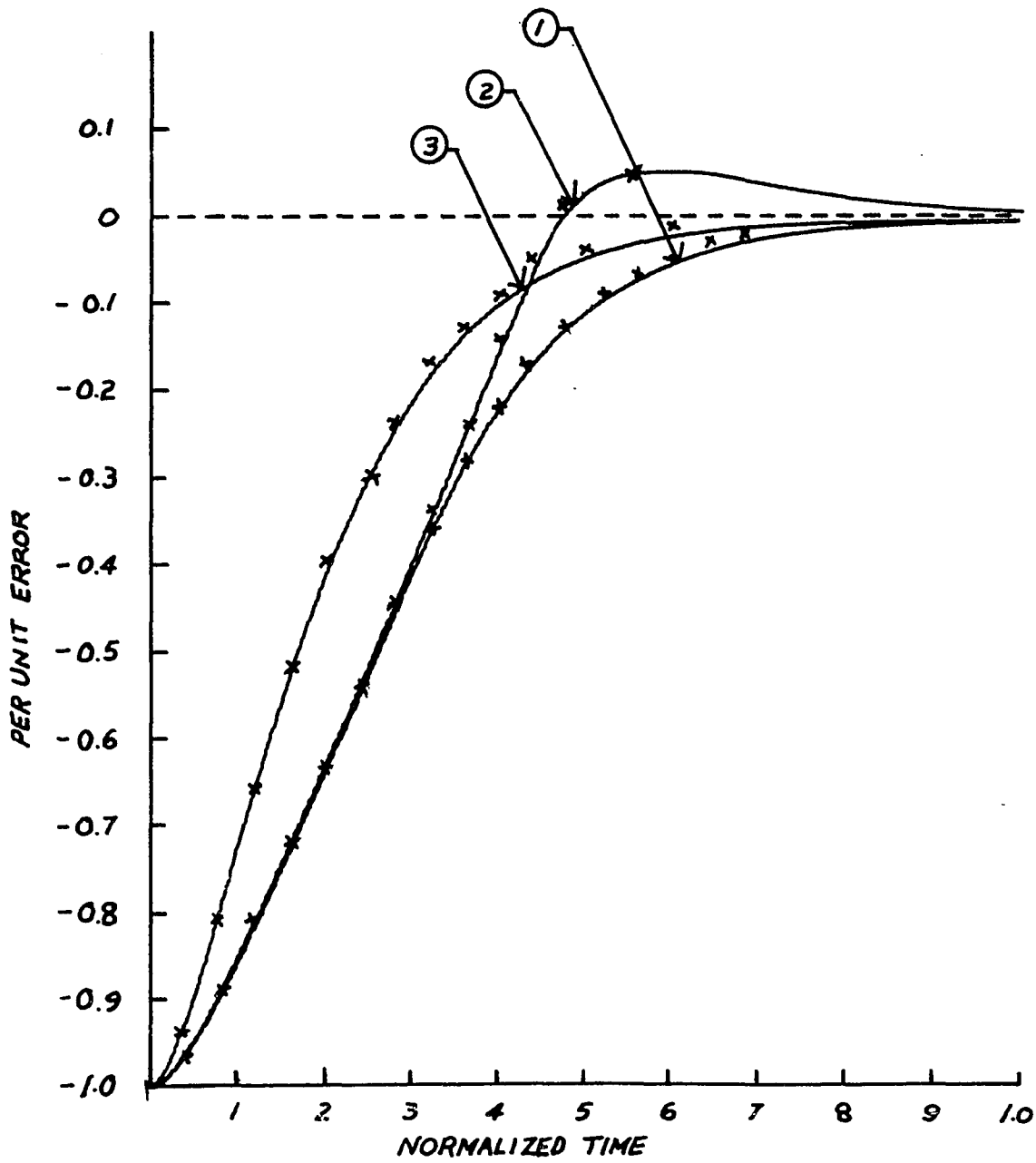

Figure 12. (1) Uncompensated, (2) compensated, and (3) linear error response recordings with superimposed calculated points for a system with damping ratio of 1.0 and initial error of 1.0

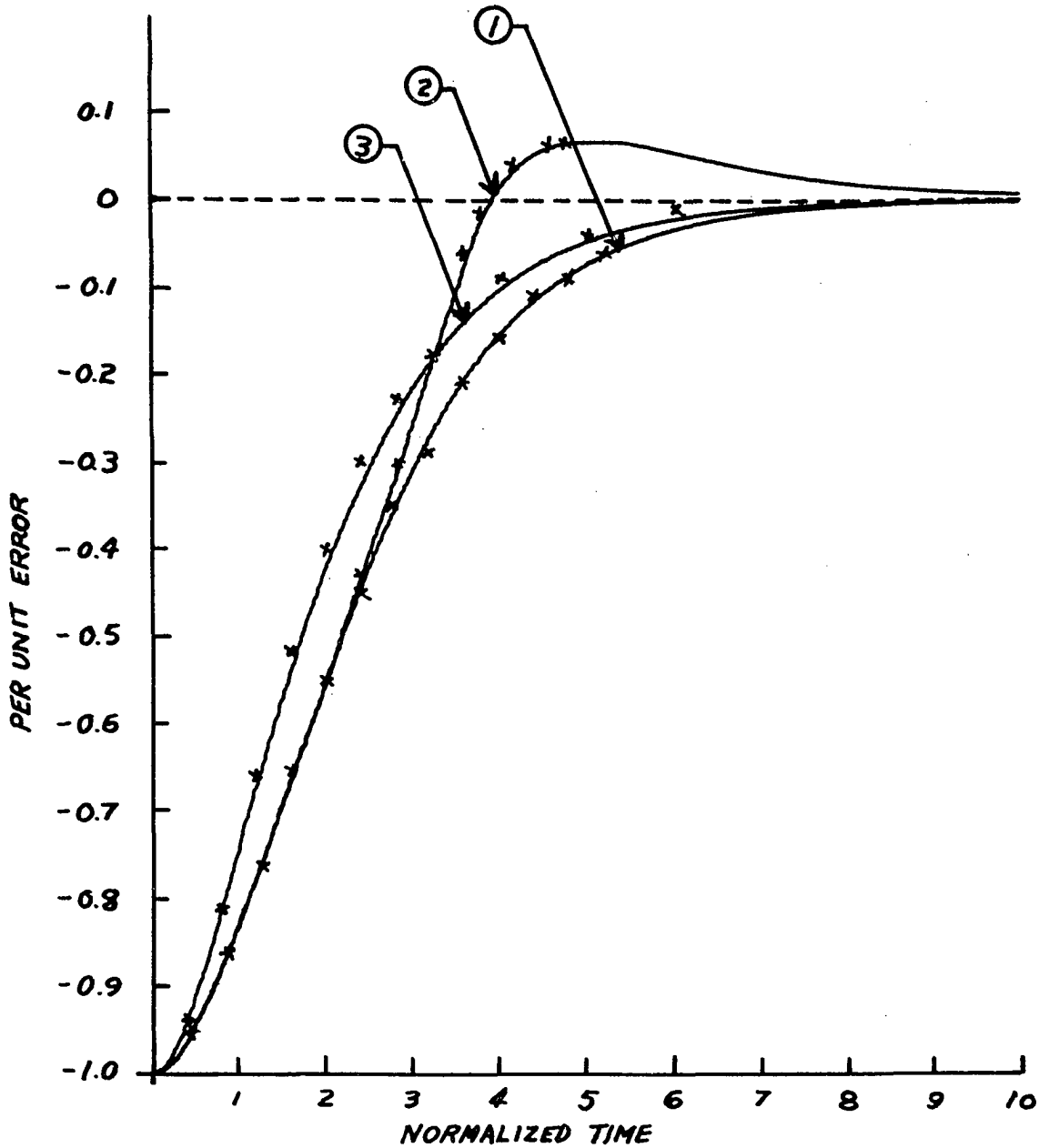

Figure 13. (1) Uncompensated, (2) compensated, and (3) linear error response recordings with superimposed calculated points for a system with damping ratio of 1.0 and initial error of 0.8

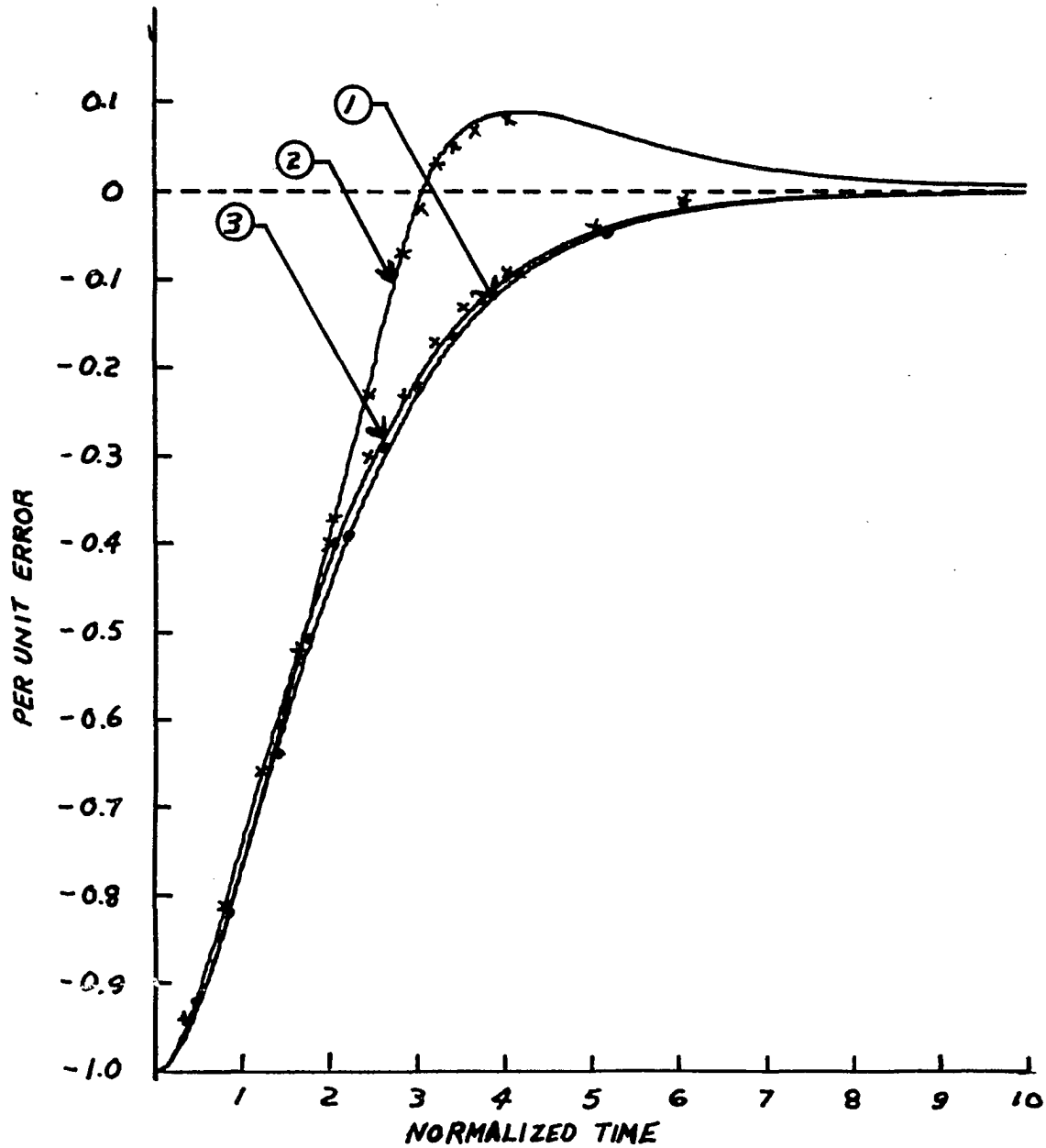

Figure 14. (1) Uncompensated, (2) compensated, and (3) linear error response recordings with superimposed calculated points for a system with damping ratio of 1.0 and initial error of 0.6

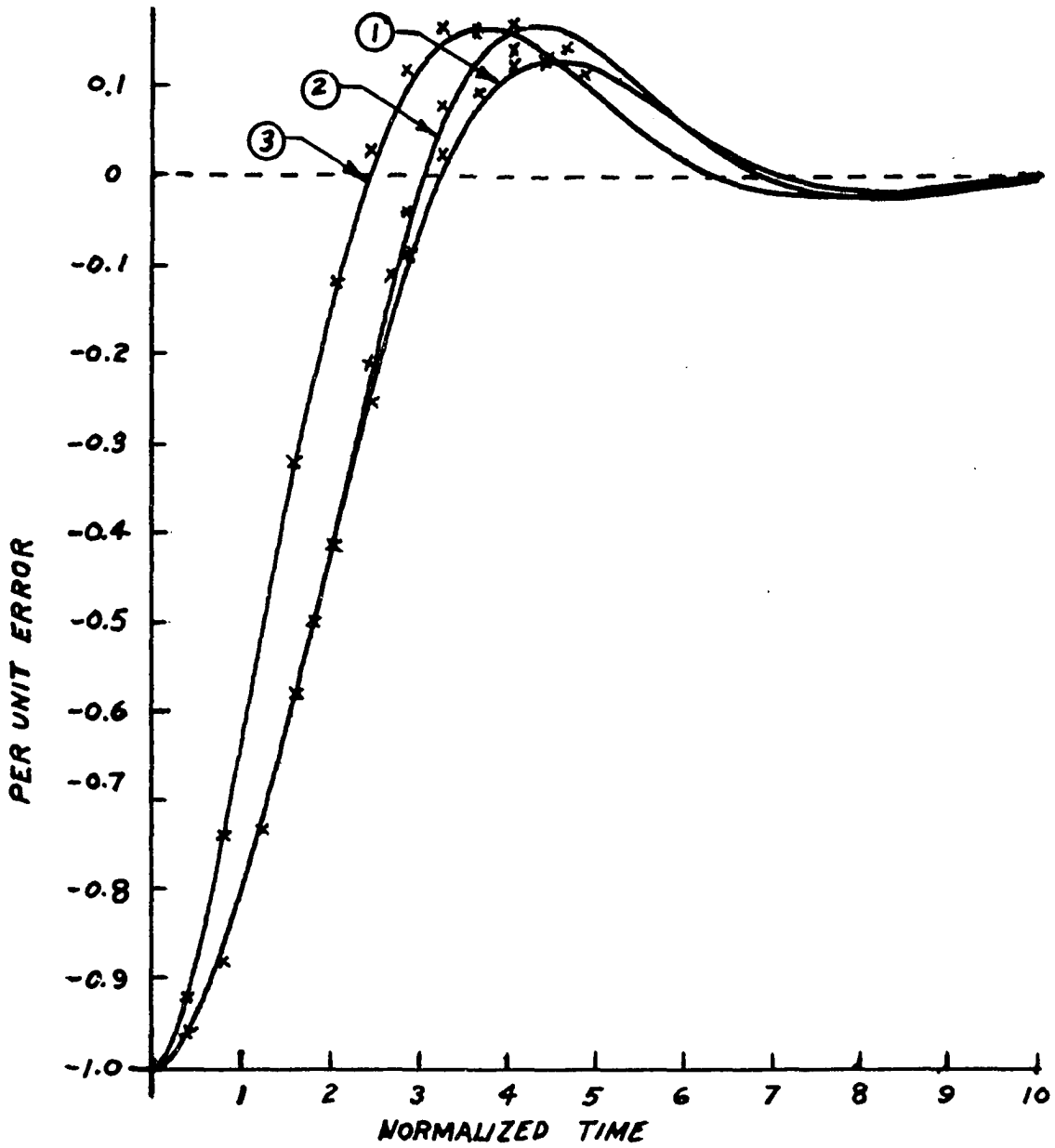

Figure 15. (1) Uncompensated, (2) compensated, and (3) linear error response recordings with superimposed calculated points for a system with damping ratio of 0.5 and initial error of 1.0

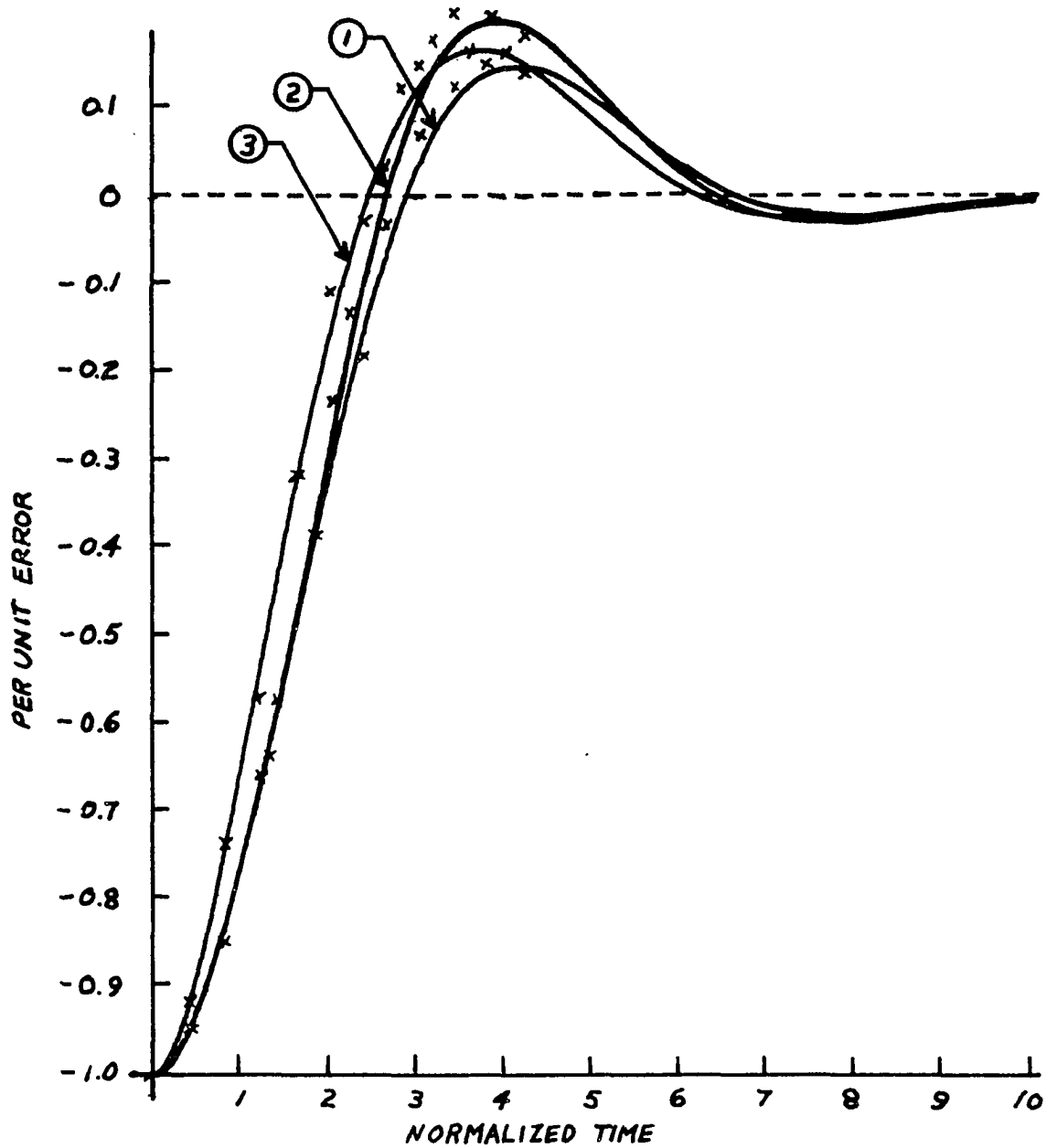

Figure 16. (1) Uncompensated, (2) compensated, and (3) linear error response recordings with superimposed calculated points for a system with damping ratio of 0.5 and inittial error of 0.8

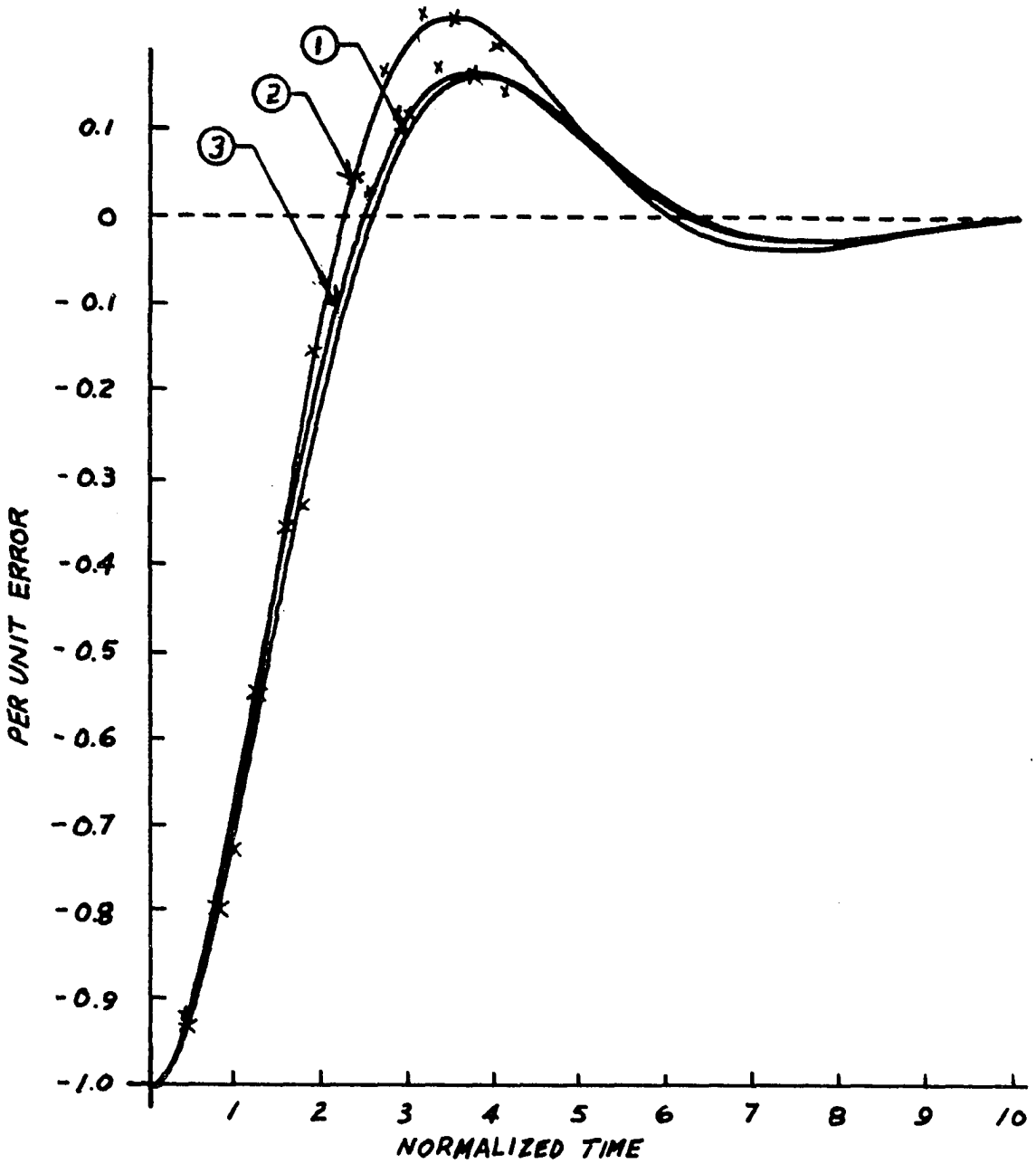

Figure 17. (1) Uncompensated, (2) compensated, and (3) linear error response recordings with superimposed calculated points for a system with damping ratio of 0.5 and initial error of 0.6

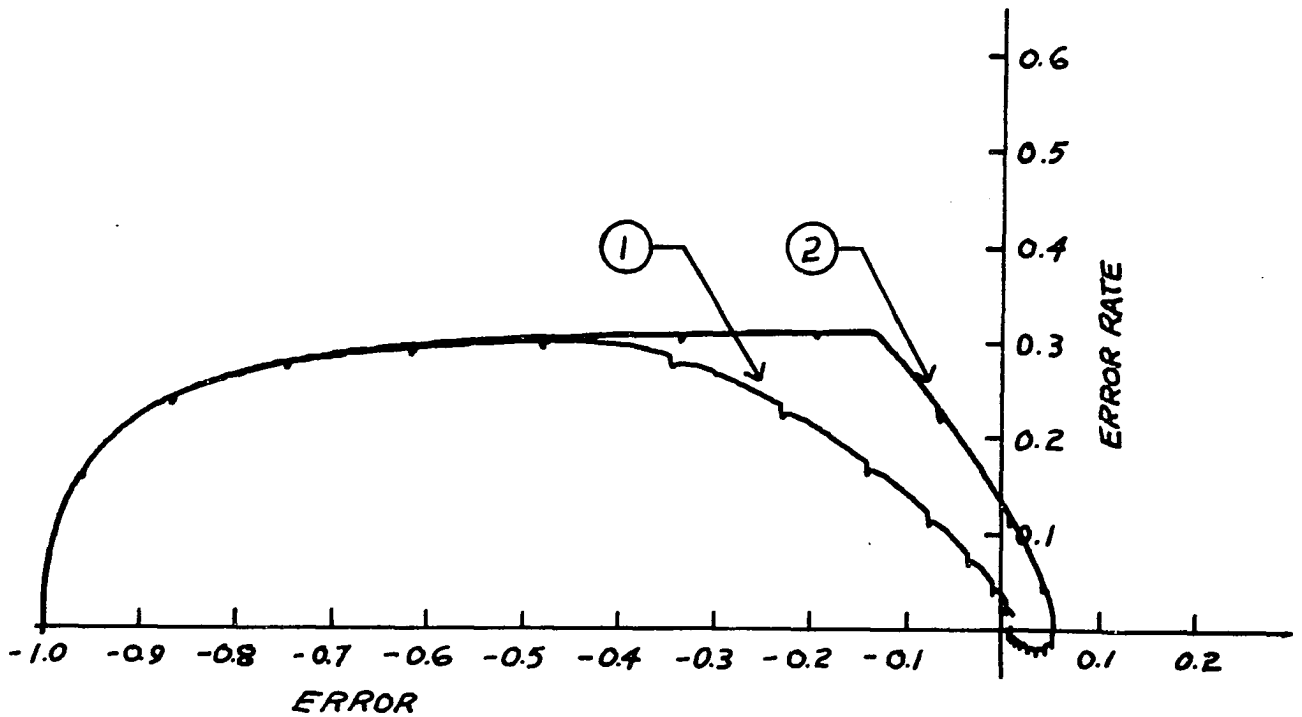

Figure 18. (1) Uncompensated and (2) compensated phase-plane trajectories for system with damping ratio of 0.8 and initial error of 1.0 (timing marks at 0.5-second intervals)

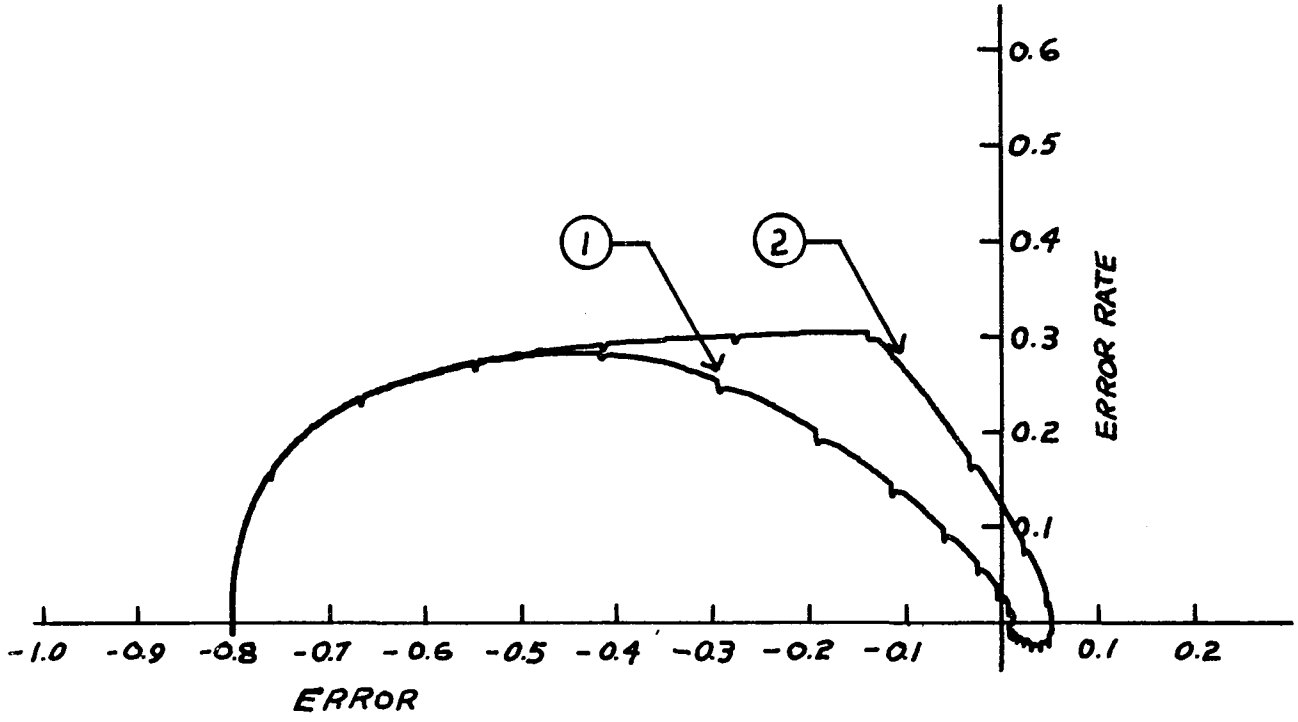

Figure 19. (1) Uncompensated and (2) compensated phase-plane trajectories for system with damping ratio of 0.8 and initial error of 0.8 (timing marks at 0.5-second intervals)

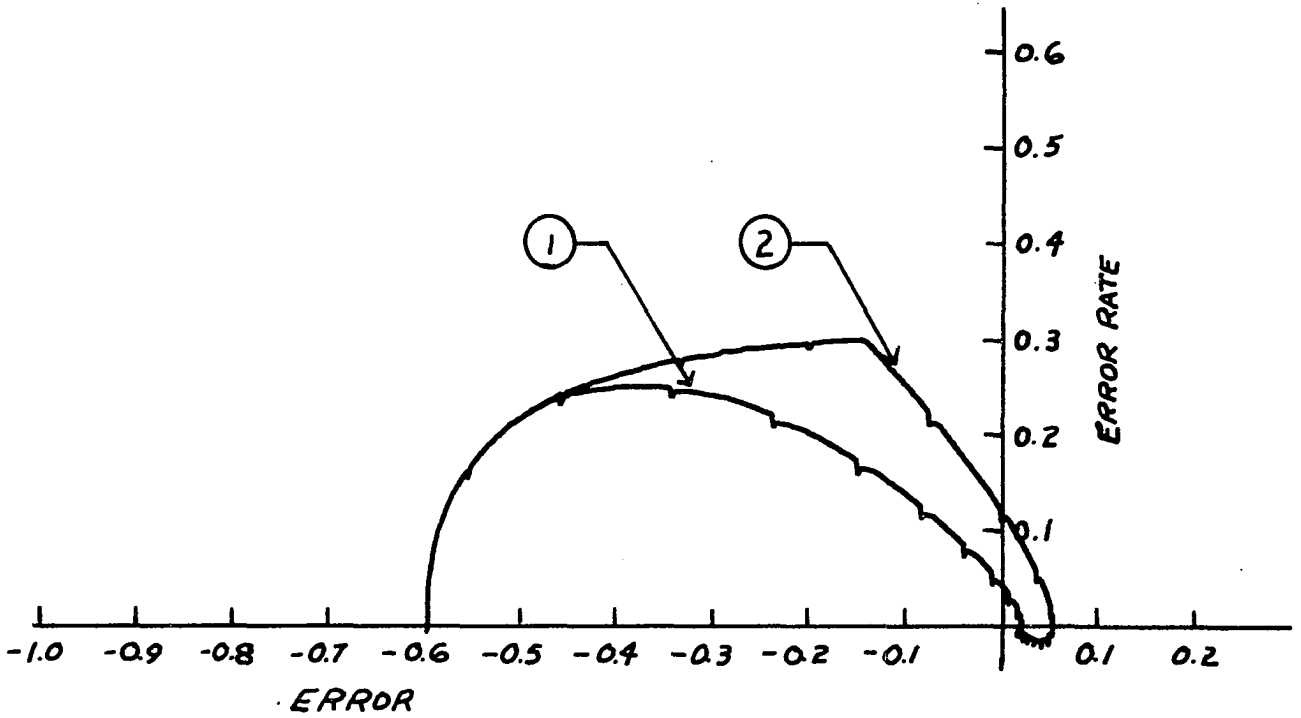

Figure 20. (1) Uncompensated and (2) compensated phase-plane trajectories for system with damping ratio of 0.8 and initial error of 0.6 (timing marks at 0.5-second intervals)

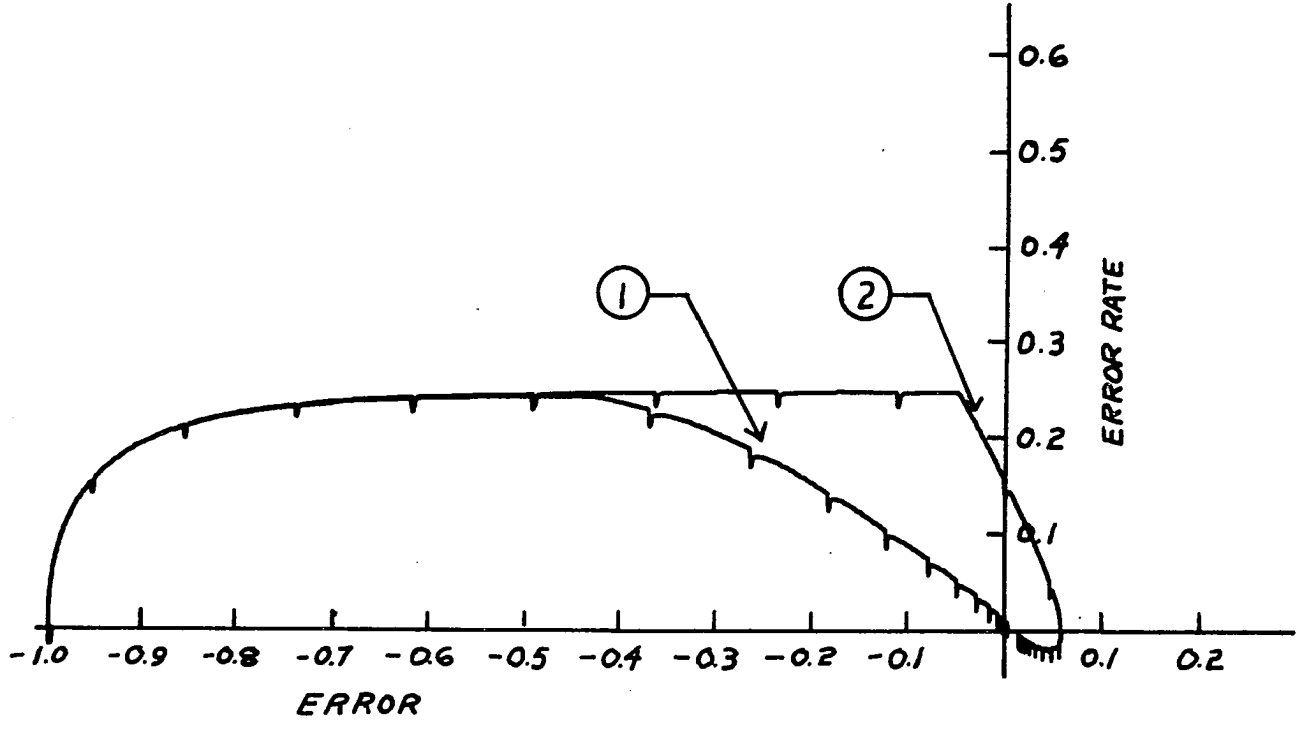

Figure 21. (1) Uncompensated and (2) compensated phase-plane trajectories for system with damping ratio of 1.0 and initial error of 1.0 (timing marks at 0.5-second intervals)

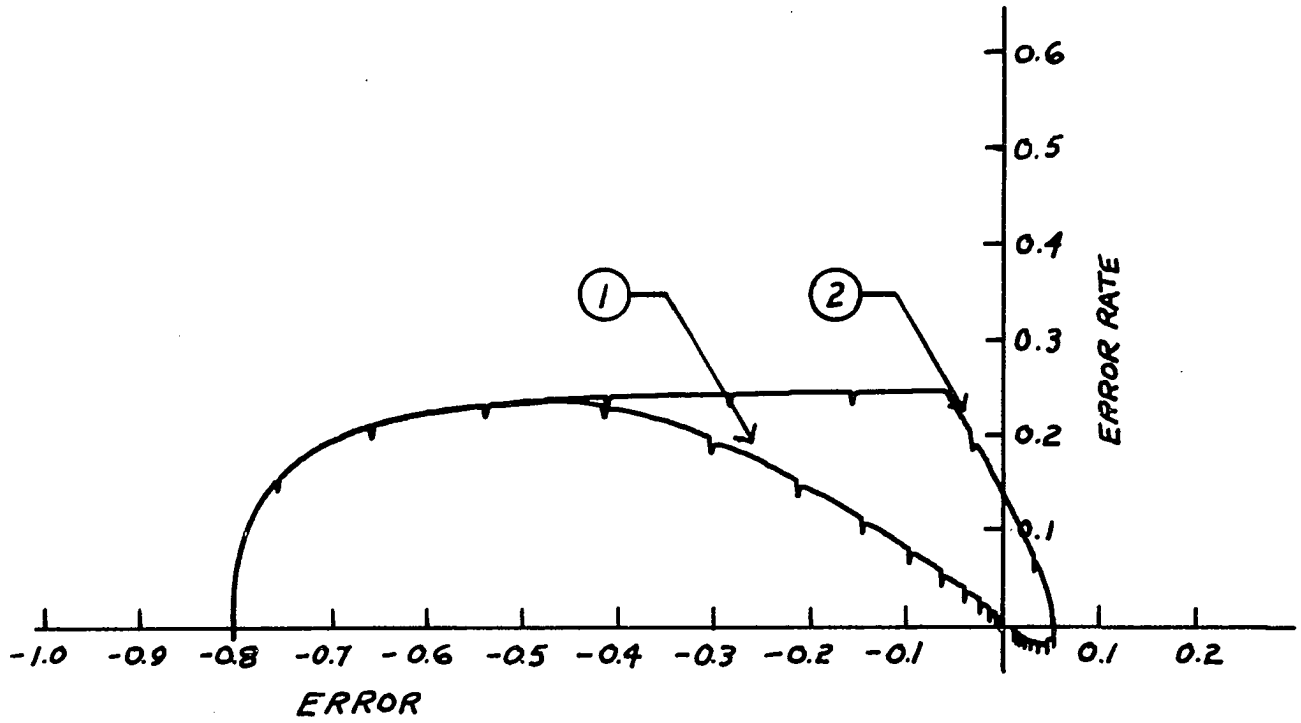

Figure 22. (1) Uncompensated and (2) compensated phase-plane trajectories for system with damping ratio of 1.0 and initial error of 0.8 (timing marks at 0.5-second intervals)

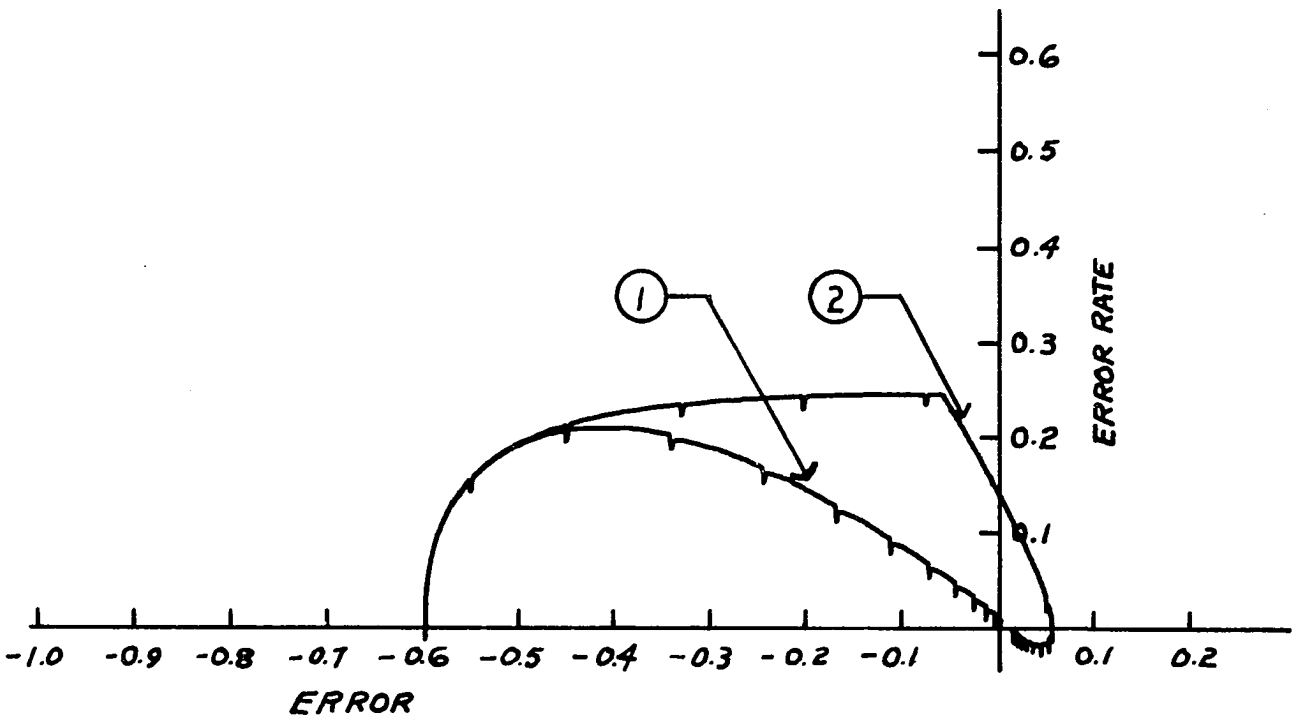

Figure 23. (1) Uncompensated and (2) compensated phase-plane trajectories for system with damping ratio of 1.0 and initial error of 0.6 (timing marks at 0.5-second intervals)

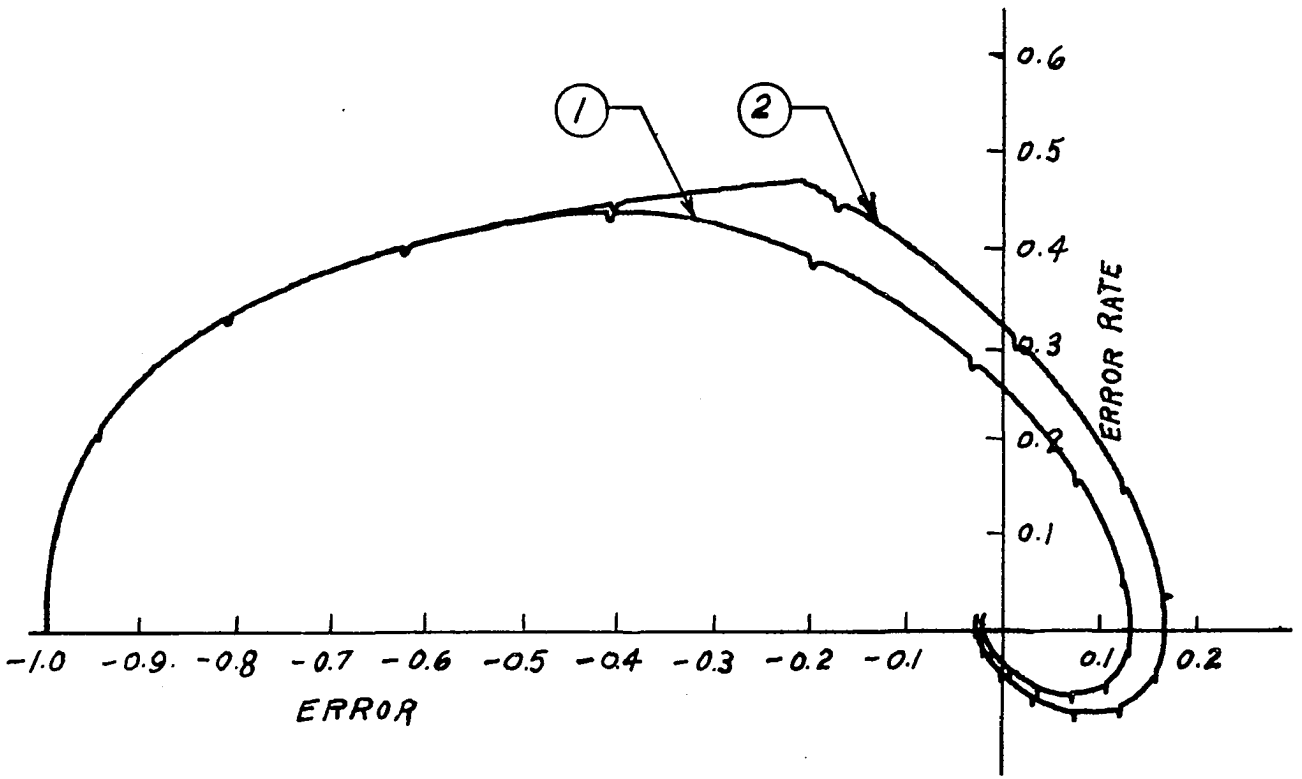

Figure 24. (1) Uncompensated and (2) compensated phase-plane trajectories for system with damping ratio of 0.5 and initial error of 1.0 (timing marks at 0.5-second intervals)

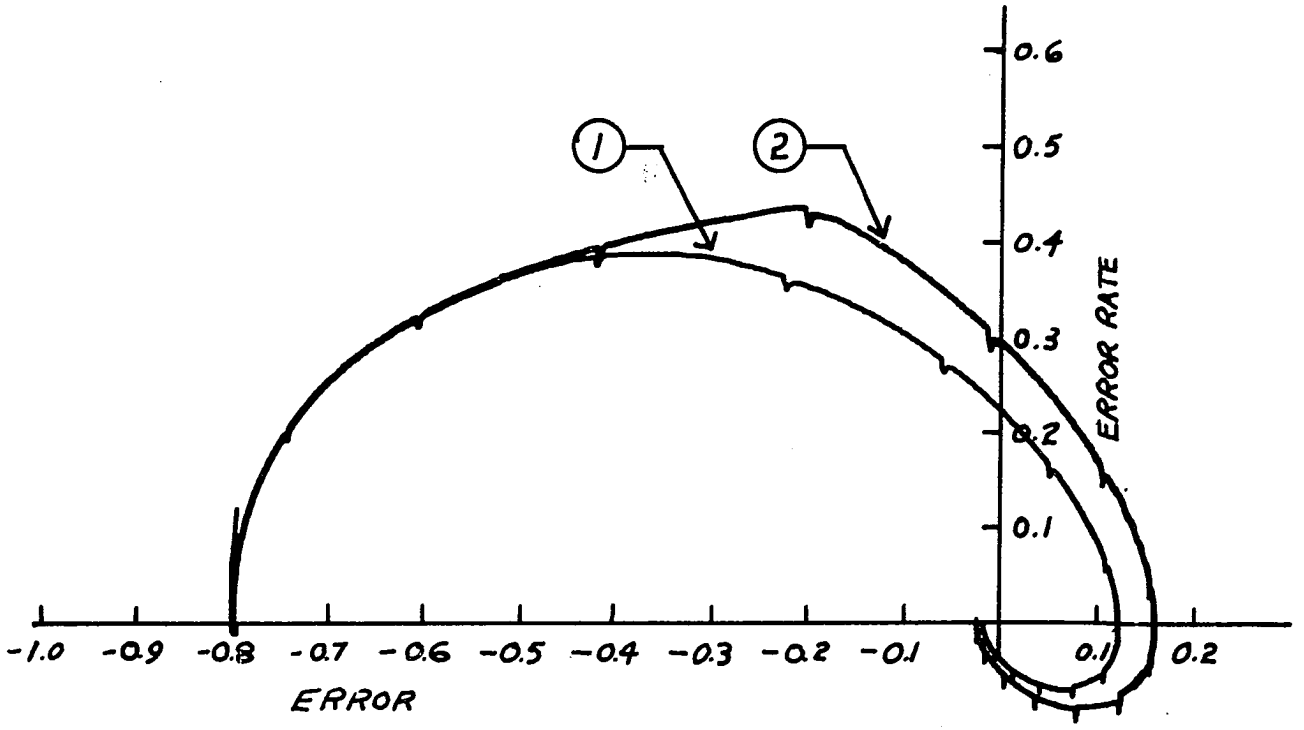

Figure 25. (1) Uncompensated and (2) compensated phase-plane trajectories for system with damping ratio of 0.5 and initial error of 0.8 (timing marks at 0.5-second intervals)

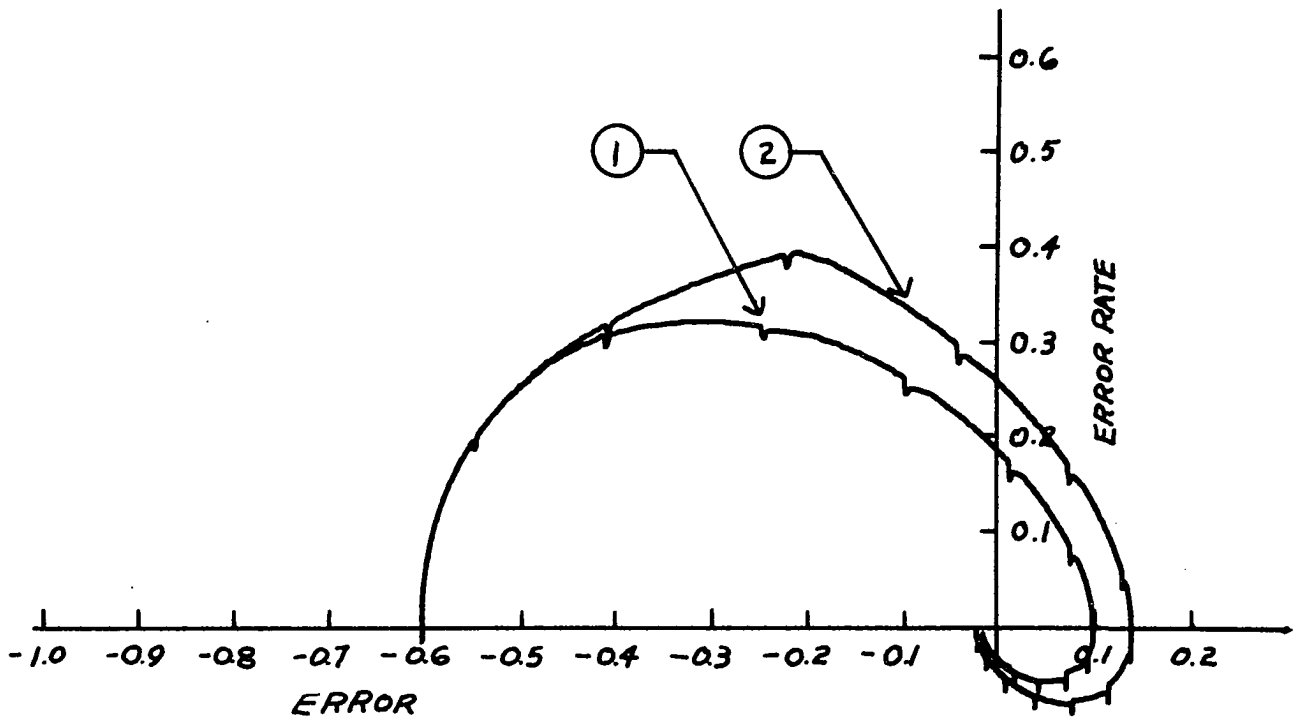

Figure 26. (1) Uncompensated and (2) compensated phase-plane trajectories for system with damping ratio of 0.5 and initial error of 0.6 (timing marks at 0.5-second intervals)

Table 10. Calculated results

Type System	Damping Ratio	Initial Error	T_d	T_r	T_s	Overshoot	% Overshoot
Linear	0.8	1.0	1.50	2.60	3.60	0.01	1.00
Uncompensated With Saturation	0.8	1.0	2.30	3.50	4.90	0.008	0.80
Compensated With Saturation	0.8	1.0	2.30	3.00	3.95	0.06	6.00
Linear	0.8	0.8	1.57	2.60	3.50	0.008	1.00
Uncompensated With Saturation	0.8	0.8	2.00	3.00	4.10	0.008	1.00
Compensated With Saturation	0.8	0.8	2.00	2.40	3.35	0.06	7.50
Linear	0.8	0.6	1.57	2.60	3.20	0.006	1.00
Uncompensated With Saturation	0.8	0.6	1.60	2.65	3.30	0.006	1.00
Compensated With Saturation	0.8	0.6	1.50	2.00	2.50	0.03	5.00

Table 11. Calculated results

Type System	Damping Ratio	Initial Error	T_d	T_r	T_s	Overshoot	% Overshoot
Linear	1.0	1.0	1.75	3.50	5.00	0	0
Uncompensated With Saturation	1.0	1.0	2.60	4.40	6.30	0	0
Compensated With Saturation	1.0	1.0	2.60	3.40	4.50	0.05	5.00
Linear	1.0	0.8	1.75	3.50	4.50	0	0
Uncompensated With Saturation	1.0	0.8	2.20	3.90	5.10	0	0
Compensated With Saturation	1.0	0.8	2.20	2.85	3.60	0.05	6.25
Linear	1.0	0.6	1.75	3.50	4.30	0	0
Uncompensated With Saturation	1.0	0.6	1.80	3.50	4.31	0	0
Compensated With Saturation	1.0	0.6	1.70	2.02	2.80	0.05	8.33

Table 12. Calculated results

Type System	Damping Ratio	Initial Error	T_d	T_r	T_s	Overshoot	% Overshoot
Linear	0.5	1.0	1.30	1.70	5.4	0.17	17.0
Uncompensated With Saturation	0.5	1.0	1.80	2.20	6.00	0.13	13.0
Compensated With Saturation	0.5	1.0	1.80	2.00	6.00	0.17	17.0
Linear	0.5	0.8	1.30	1.70	5.30	0.136	17.0
Uncompensated With Saturation	0.5	0.8	1.60	1.90	5.80	0.12	14.0
Compensated With Saturation	0.5	0.8	1.60	1.80	5.7	0.152	19.0
Linear	0.5	0.6	1.30	1.70	5.00	0.102	17.0
Uncompensated With Saturation	0.5	0.6	1.50	1.65	5.00	0.102	17.0
Compensated With Saturation	0.5	0.6	1.50	1.50	5.00	0.132	22.0

C. Conclusions

Both the calculated results and the results of analog computer simulation point to the following conclusions:

1. Hysteresis compensation is most effective in systems having a large damping ratio. In fact, Figures 12, 13, and 14 and Table 11 show that for a critically damped system it is possible to have a faster settling time for the saturated system with compensation than is possible if no saturation is present.
2. Improvement in speed of response is made at the expense of increased overshoot.
3. The upper bound on overshoot is controlled by the dropout point of the compensator and can be set rather precisely.
4. The hysteresis compensator is most effective when the initial error conditions just slightly exceed the saturation level.
5. The fastest allowable response time for a given system can be obtained by setting the dropout point of the compensator as low as possible without exceeding the limits on overshoot.

It has previously been shown that a second-order system with hard saturation and a hysteresis compensator can be analyzed for design purposes either by graphical methods or by using linear techniques. The analysis by linear methods is made possible by the fact that the input-output characteristic of the amplifier and of the amplifier-compensator combination can be broken up into linear sections. The graphical method is subject to no such limitations and thus could be applied to any nonlinearity of the saturation type.

III. QUASI-OPTIMIZATION USING HYSTERESIS ELEMENTS

A possible step in determining the usefulness of a hysteresis element for improving the step response of a position-control system with hard saturation would be to determine the time-optimum response of the system and to attempt, through the use of the hysteresis compensator, to obtain a trajectory as near as possible to the time-optimum trajectory. The time-optimal system has been shown by a number of writers, among them Bellman (8), Kalman (5), and Pontryagin (9), to be a system that employs its maximum available effort at all times and switches the polarity of its effort at the optimum moments.

Before an attempt is made to improve the response time of a system, it might be helpful to investigate how close its response is to the response of a similar time-optimal system. If the step response of a given system is already almost optimal for the elements used in the system; it would be difficult, if not impossible, to make a noticeable improvement short of completely re-designing the control elements.

To illustrate the above point a comparison will be made between a second-order servomechanism with hard saturation and a similar system working in conjunction with a time-optimal-relay controller. The two block diagrams are shown in Figures 27a and 27b.

In the saturated system the amplifier saturates at an error of 0.5 units. The controller of the time-optimal system has an output of 0.5 units and changes sign as a function of e and $\dot{e}$ in such a way that the system moves with maximum speed to the switching boundary at which time the polarity of the motor input is reversed to decelerate the system along the

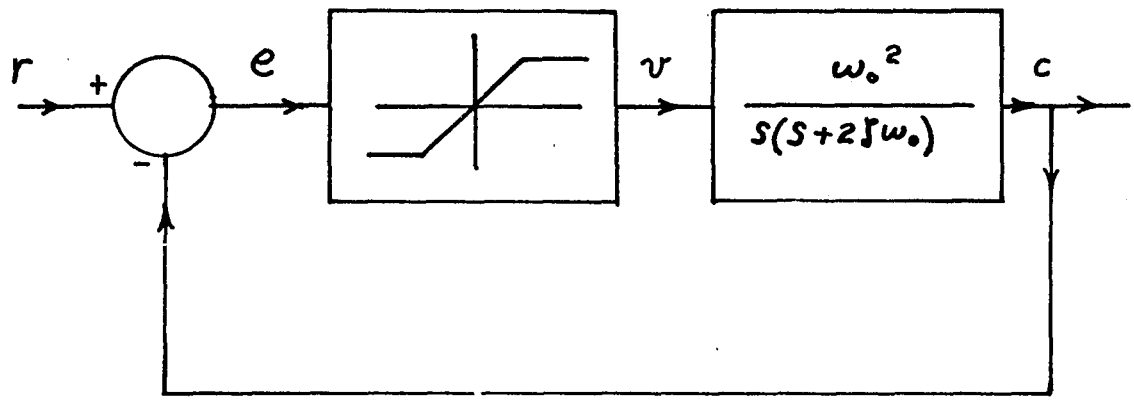

Figure 27a. Saturated system

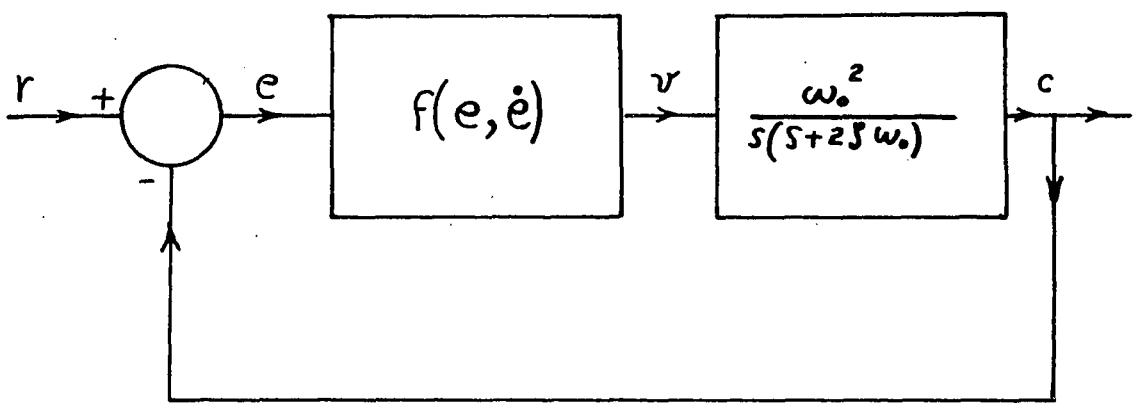

Figure 27b. Time-optimal system

optimum trajectory to the origin of the phase-space. A more complete discussion of time-optimal systems can be found in most texts on nonlinear controls, among them are texts by Gibson (10), Thaler and Pastel (11), and Cosgrift (12). The phase-plane trajectory for the saturated system is plotted in the same manner as was done in Section II. The time-optimal system is described by Equation 6 during the time from the initiation of the problem until it reaches the switching trajectory, at which time the polarity of the controller output is reversed. During deceleration the time-optimal system is described by the differential equation

$$\ddot{e} + 2\zeta\dot{e} = -0.5 \qquad (7)$$

It can be seen that Equation 7 is the same as Equation 6 except that the sign of the driving function is reversed. It is now convenient to plot the deceleration trajectory by Pell's method (7) or by any other method that is desired. It is known that the optimum deceleration trajectory ends at the origin of the phase-space and therefore it is convenient to plot the deceleration trajectory backwards starting at the origin.

The trajectories for the uncompensated system, the hysteresis-compensated system, and the time-optimal system are shown in Figure 28. The trajectories for the uncompensated system and the time-optimal system are seen to be identical in the region where the error is larger than 0.5 units. In the region where the error is between 0.5 units and zero, the trajectory of the time-optimal system passes through the points B, D , and O and lies above the linear portion of the trajectory of the uncompensated system. Therefore the optimal system traverses its trajectory from point

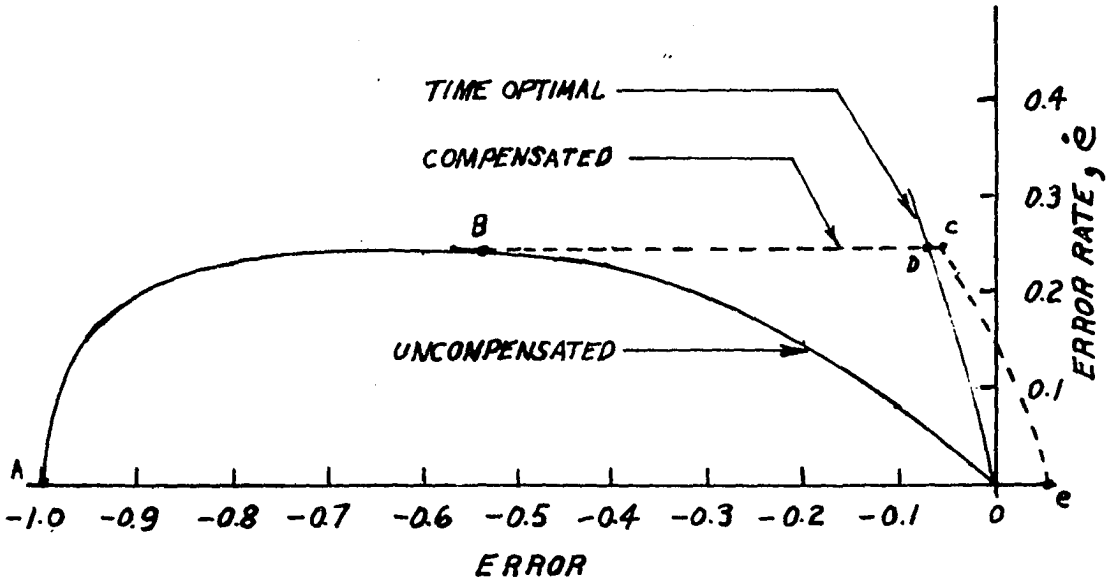

Figure 28. Comparison of uncompensated, compensated, and time optimal trajectories for system with damping ratio of 1.0

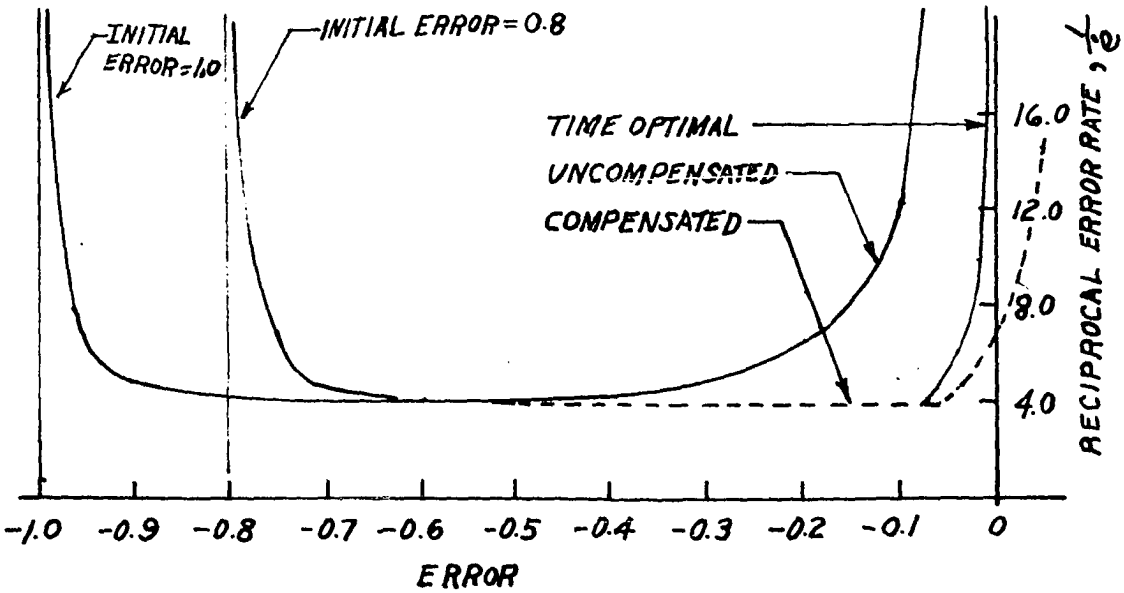

Figure 29. Curves of reciprocal error rate versus error for uncompensated, compensated, and time optimal system with damping ratio of 1.0

B to point O in less time than does the uncompensated system. Since the two trajectories are identical from point A to point B, the maximum time that could be gained by any compensation method is the difference in time required to traverse trajectories BDO and BO.

The time required for the system to move from a point designated e_1 to a point designated e_2 can be determined in the following manner: By definition

$$\dot{e} = \frac{de}{dT} \tag{8}$$

It follows that

$$dT = \frac{de}{\dot{e}} \tag{9}$$

and thus we can obtain

$$T = \int_{e_1}^{e_2} \frac{1}{\dot{e}} \, de \tag{10}$$

Graphically, Equation 10 can be interpreted as the area, between the lines e_1 and e_2, which lies under the curve of $\frac{1}{\dot{e}}$ versus e. Figure 29 shows such curves for the systems of Figures 27a and 27b with initial errors of 1.0 units and 0.8 units. The settling time of the system can be computed as the area under the curves that lies between the initial error and an error of 0.05 units. It can be seen that if the initial error is large enough so

that the system is velocity-limited, the difference between the settling times of the two systems is a constant. If the difference in response time is calculated on a percentage basis, the response of the uncompensated system is more nearly optimal for very large, initial errors than for small, initial errors. In view of this fact one might expect that on a percentage basis very little can be done to improve the time response of a saturated system when the input is a very large step function. On the other hand, if the largest input step that the system is to be subjected to is only slightly above the saturation level, it may be possible to considerably shorten the response time through the use of a hysteresis compensator.

It was stated previously that the compensating device would be chosen to reduce an initial error to zero as rapidly as possible without exceeding some upper bound on overshoot as specified by the particular problem at hand. To accomplish this one might choose the dropout point of the hysteresis element to give an after-dropout trajectory as nearly like the deceleration trajectory of the optimal system as is possible without exceeding the overshoot limitations. In cases where the overshoot must be small, the after-dropout trajectory may be determined by the allowable overshoot.

If a hysteresis-element compensator is added to the system of Figure 27a and the dropout point is chosen to give a maximum overshoot of 0.05 units, the trajectory is as shown by the dotted line on Figure 28. It can be seen that this trajectory is much closer to the optimal trajectory than that of the uncompensated system. The reciprocal-velocity curve for the compensated system in Figure 29 shows that the settling times of the two systems would be very nearly the same. If the maximum overshoot of 0.05 units is tolerable, the step response of the compensated system would be

just as good for all practical purposes as the time-optimal system.

The previous comparison illustrates that for a critically-damped system with hard saturation, a hysteresis compensator can make the step response of the system very nearly optimum for input steps larger than the saturation level of the amplifier. It has been observed previously that for underdamped systems the hysteresis compensator is not nearly so effective. This fact is also revealed if one compares the underdamped system response with that of a similar time-optimal system. Figure 30 shows a comparison of the trajectories of a system having a damping ratio of 0.5 with a similar time-optimal system. For an initial error of 1.0 units the trajectory of the uncompensated system appears to be about as close an approximation to the optimum trajectory as is possible. In this case a hysteresis compensator would only serve to increase the overshoot and would increase the settling time. Curves of $\frac{1}{\dot{e}}$ versus e shown in Figure 31 corroborate the conclusions that the hysteresis compensator is not effective on greatly underdamped systems.

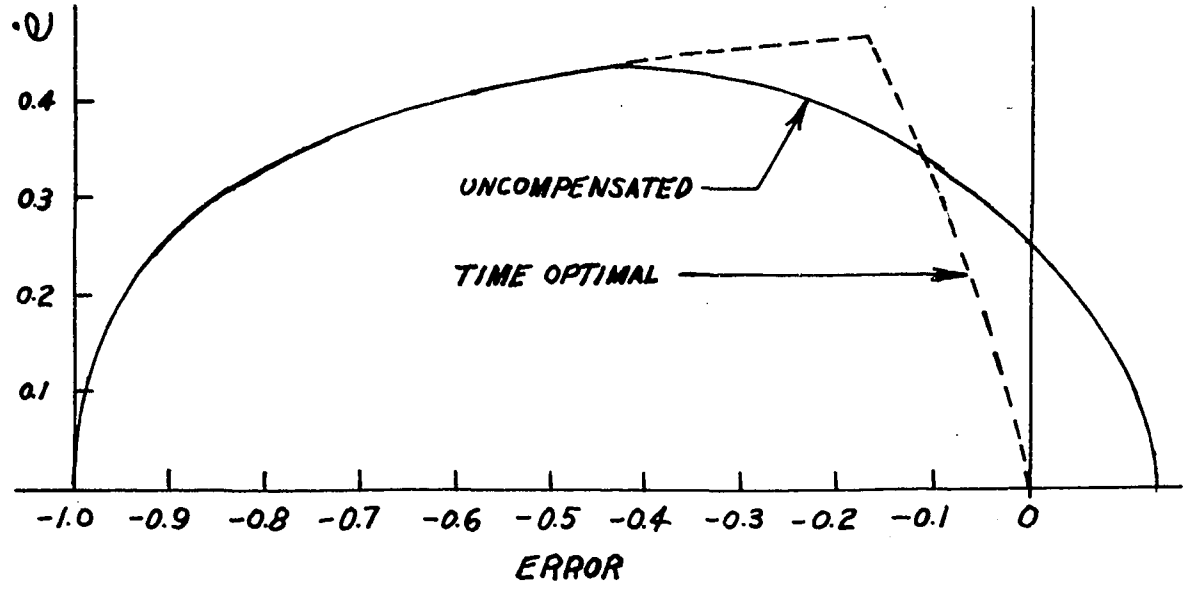

Figure 30. Comparison of compensated and time optimal trajectories for system with damping ratio of 0.5

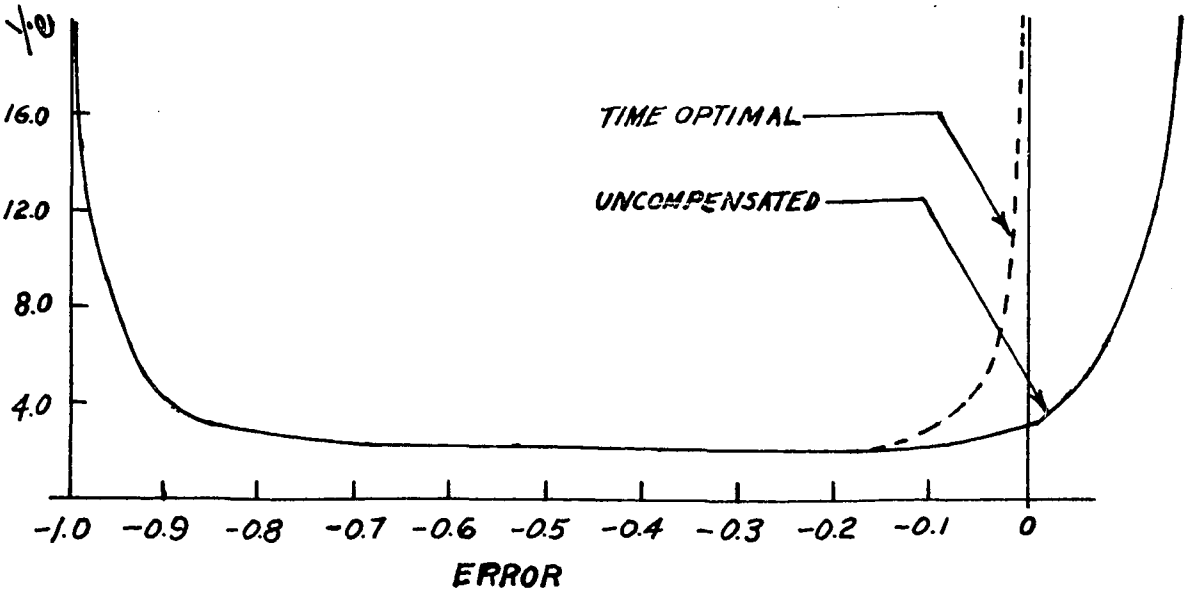

Figure 31. Curves of reciprocal error rate versus error for compensated and time optimal system with damping ratio of 0.5

IV. DESIGN OF A HYSTERESIS COMPENSATOR FOR A THIRD-ORDER SYSTEM

A. Analytical Considerations

The work done in the previous sections has dealt with the design of hysteresis compensation for second-order systems only. An obvious question would be whether the technique can be extended to include systems described by differential equations of higher than second order. If the saturating amplifier characteristic is sectionally linear or can be sufficiently closely approximated by a sectionally linear curve, the linear techniques discussed in Chapter II are valid and can be used for systems of any order. The possibility of a purely graphical procedure seems unlikely since the construction of a phase-space trajectory for a system of third or higher order is difficult. However, it would be possible to obtain a set of curves of velocity versus position (the projection of the phase-space trajectory onto the e and $\dot{e}$ axes) similar to trajectories 1, 2, and 3 of Figure 3. Such curves could then be used to choose the optimum dropout point for the compensator just as was done in the second-order systems previously discussed.

Another approach to the problem of analyzing a third-order system for the purpose of designing a compensator would be to make use of the fact that the characteristics of a large number of higher order systems are determined largely by the location of the control poles in the complex s-plane (13). If it can be assumed that the system will behave very similarily to an equivalent second-order system, a nonlinear compensator can be designed whose dropout point is determined as illustrated in the pre-

vious examples. While this approach is certainly not rigorous, it might be useful for making a preliminary design.

B. Use of the Analog Computer to Design a Hysteresis Compensator for a Third-Order System

An attempt will be made to design a hysteresis compensator for a third-order position control system that will make the system as close as possible to the time-optimal system as discussed in Section III. Bogner and Kazda (14) have shown that under certain conditions, n-1 switching boundaries are required for time-optimum, transient response to a step-function input for a stable nth-order system with real roots. Kalman (5) states that, in practice, the first reversal of polarity is the most significant for most systems and that usually a very good approximation to the optimal response can be obtained by having one reversal of polarity and providing a region of linear operation near the origin of the phase-space. The other optimal reversals usually occur in that region. If the system under consideration is heavily damped, it quickly reaches its velocity limit. During the time when the system is velocity-limited the acceleration is zero and the phase-space trajectory lies in the e, $\dot{e}$ plane at the time when the first switching boundary is reached. It follows that an approximation can be made to the optimum deceleration trajectory by setting the initial conditions of the open-loop system at the proper value and applying a constant voltage of the correct polarity and magnitude to the input. The velocity-versus-position curve is then recorded using a x-y plotter. Usually after a few trials, the initial conditions can be set to obtain a trajectory that passes through the origin. This trajectory will be

assumed to be a good approximation to the optimal trajectory.

The system to be analyzed consists of a linear plant having a transfer function of

$$G(s) = \frac{0.56}{s\,(s+1.2)(s+2.1)} \qquad (11)$$

in series with a saturating amplifier of the same type as shown in Figure 2. The parameters were chosen to give a system very nearly critically damped in order to illustrate the method under conditions which are favorable to the use of a hysteresis compensator. The system was simulated on an analog computer and the approximate optimal deceleration trajectory was obtained by setting the initial values of position and velocity and providing a constant forward-loop voltage equal to the saturation voltage in such a way as to drive the system trajectory through the origin along an approximately optimal trajectory. This trajectory was recorded on an x-y plotter and is shown in Figure 32.

The second step is to record on the same set of axes compensated trajectories with several different dropout points. In Figure 32 trajectories are recorded for dropout points of 0.1, 0.125 and 0.175 units. An inspection of Figure 32 reveals that of the three after-dropout trajectories the trajectory for a dropout point of 0.125 units seems to most closely approximate the optimal trajectory.

A dropout point of 0.125 units will be chosen. The time responses for the uncompensated system, the compensated system, the linear system with no saturation present, and the approximate time-optimal system are shown

in Figure 33.

The results show that for this system it was possible to design a hysteresis compensator that gave results very near to those of the time-optimal system. The results also show that the effect of the hysteresis compensator on a third-order system is essentially the same as on a second-order system. The chief difference in the design procedure is that direct graphical calculations cannot be used for the third-order system.

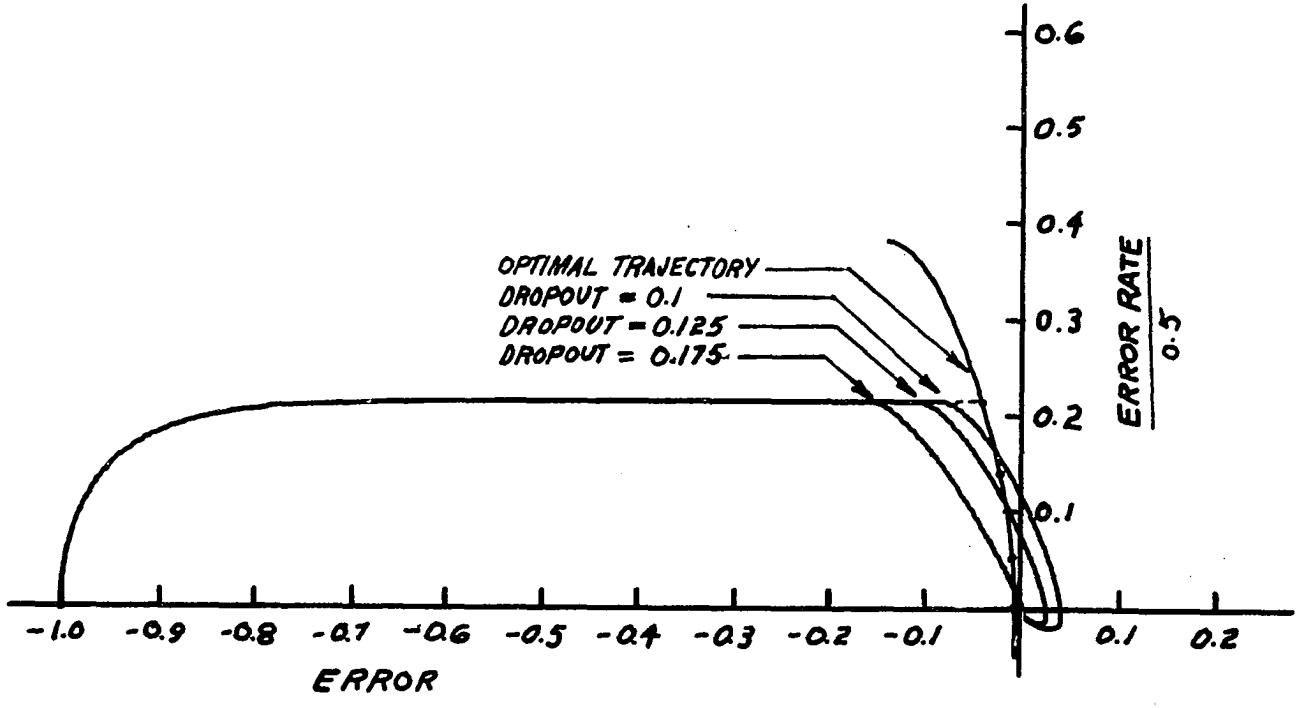

Figure 32. Recorded curves of error rate versus error used for determination of quasi-optimum dropout point for a third order system

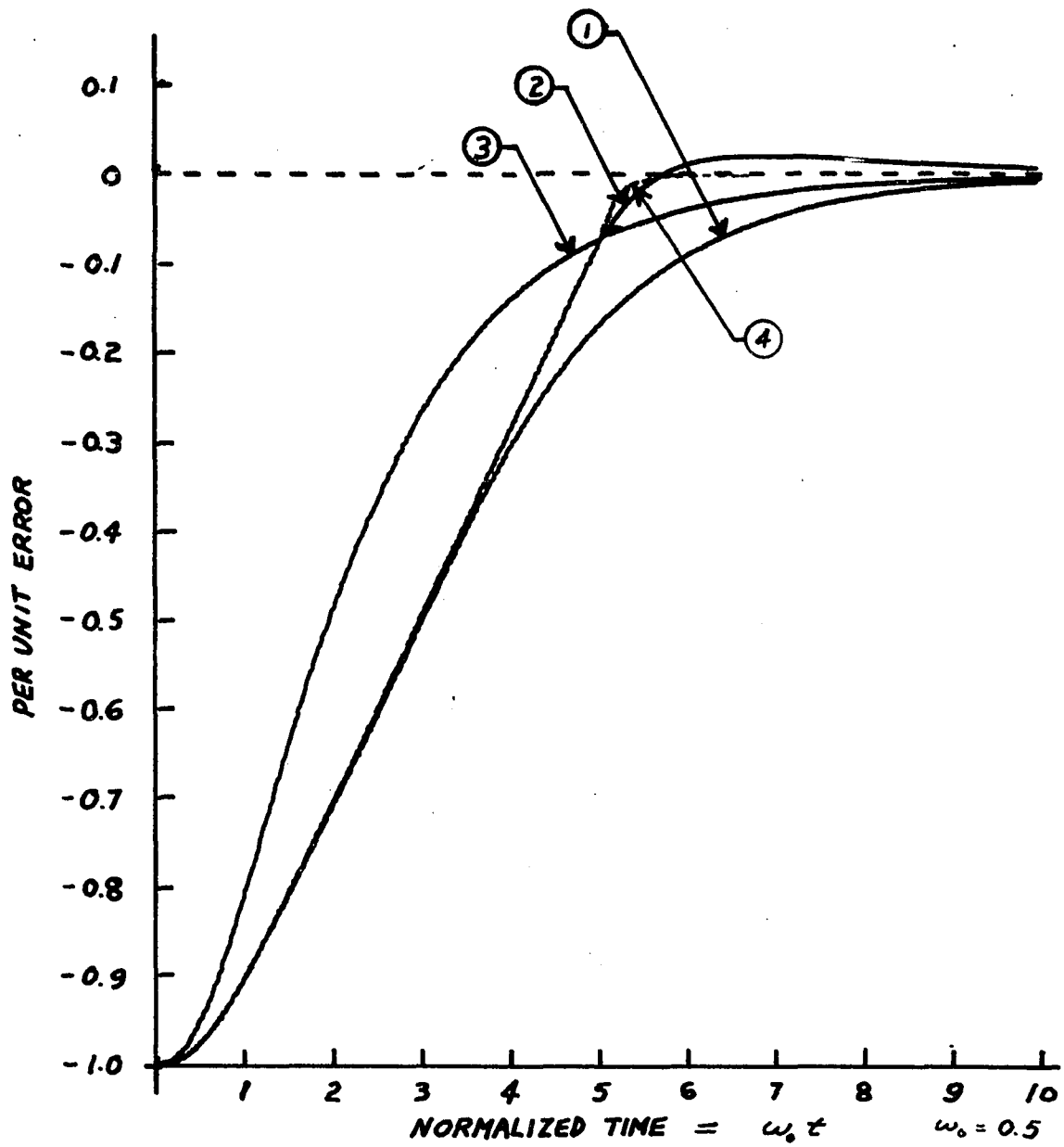

Figure 33. Error responses for third order system: (1) uncompensated, (2) compensated, (3) linear system, and (4) optimal

V. RANDOM SIGNALS APPLIED TO A HYSTERESIS-COMPENSATED SYSTEM

A. Calculation of the Output Probability Density Distribution

An amplitude-nonlinear element such as discussed in this dissertation introduces distortion of the input signal. Passing a random signal through a nonlinear device changes the probability density distribution of the output with respect to that of the input. Analysis of the performance of the hysteresis-compensated limiter with random inputs is complicated by the fact that the input-output characteristic of the hysteresis element is not a single-valued function. The problem here seems to resolve itself into finding the output probability density distribution of the nonlinear element if one is given the probability density distribution of the input. This has been done by a number of authors for a single-valued nonlinearity but is considerably more difficult when the nonlinearity is double-valued.

Let us consider a nonlinearity of the hysteresis-type such as shown in Figure 34. It will be assumed that the input to the hysteresis element has a probability density distribution, $P(y)$, and the probability density distribution of the output, $P(z)$, will be calculated. The input probability density distribution will be divided into two portions, $P_U(y)$ and $P_L(y)$, each of which sees a different, single-valued nonlinearity. $P_U(y)$ sees the nonlinearity of Figure 35 while $P_L(y)$ sees the nonlinearity of Figure 36.

The ratio of $P_U(y)$ to $P_L(y)$ is given by the following equation

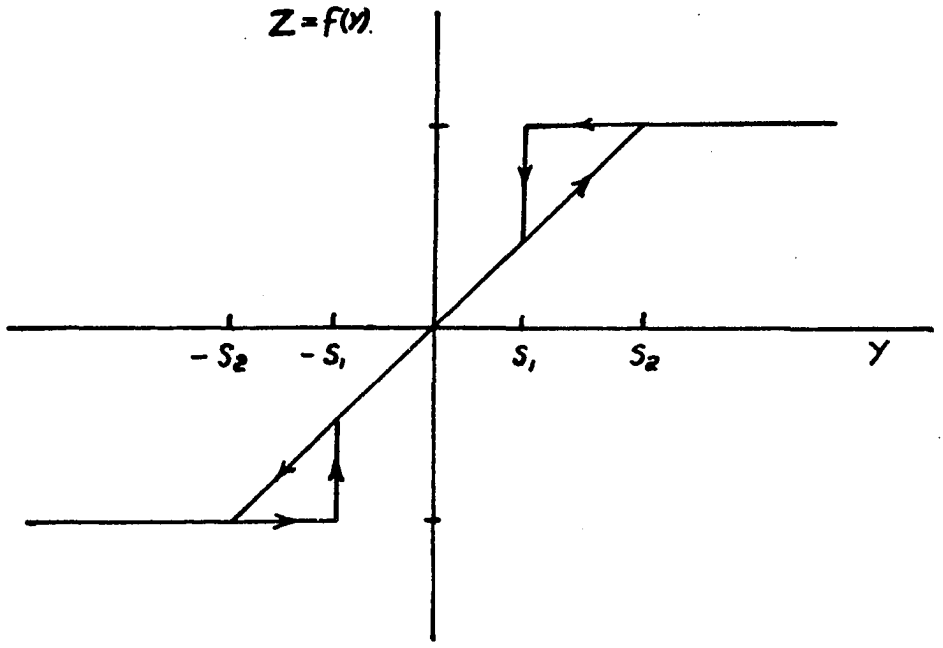

Figure 34. Input-output characteristic of hysteresis compensated limiter

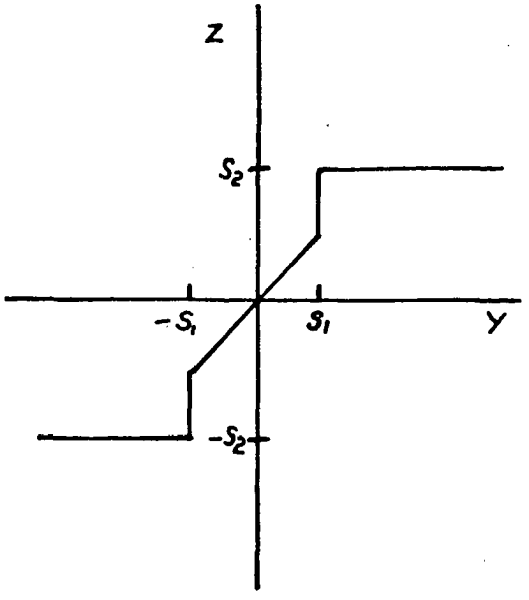

Figure 35. Nonlinearity seen by $P_u(y)$

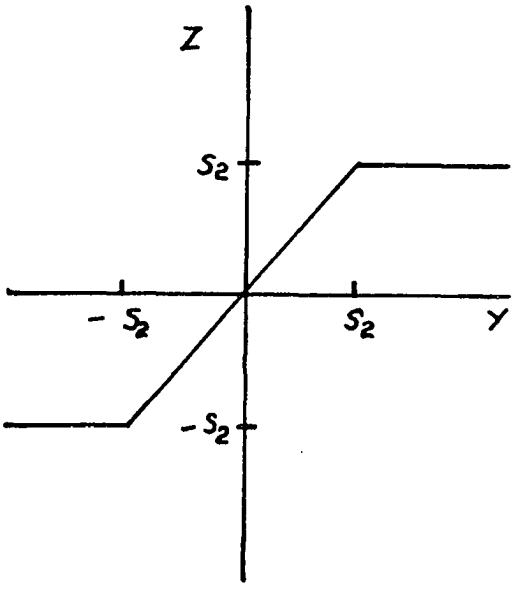

Figure 36. Nonlinearity seen by $P_L(y)$

$$\frac{P_U(y)}{P_L(y)} = \frac{\int_{S_2}^{\infty} P(y)\ dy}{\int_{-\infty}^{S_1} P(y)\ dy} \tag{12}$$

The above ratio will be defined as m.

Since

$$P(y) = P_U(y) + P_L(y) \tag{13}$$

the following relationships can be obtained.

$$P_L(y) = \left(\frac{1}{1 + m} \right) P(y) \tag{14}$$

and

$$P_U(y) = \left(\frac{m}{1 + m} \right) P(y) \tag{15}$$

The output probability density distribution, P(z), will also be expressed as the sum of the output probability density distributions from Figure 35, $P_U(z)$, and Figure 36, $P_L(z)$. $P_U(z)$ and $P_L(z)$ are related to P(y) by the following equations.

$$P_U(z) = \begin{cases} \frac{m}{1+m} \; P(y) & 0 < z < S_1 \\ \frac{m}{1+m} \int_{S_1}^{\infty} P(y)\, dy \;\; \delta(z - S_2) & z \geq S_2 \end{cases} \tag{16}$$

Where $\delta(z - S_2)$ is the Dirac delta function.

$$P_L(z) = \begin{cases} \frac{1}{1+m} \; P(y) & 0 < z < S_2 \\ \frac{1}{1+m} \int_{S_2}^{\infty} P(y)\, dy \;\; \delta(z - S_2) & z \geq S_2 \end{cases} \tag{17}$$

The output probability density distribution will be the sum of $P_U(z)$ and $P_L(z)$ or

$$P(z) = \begin{cases} P(y) & 0 < z < S_1 \\ \frac{1}{1+m} \; P(y) & S_1 < z < S_2 \\ \left[\frac{m}{1+m} \int_{S_1}^{\infty} P(y)\, dy + \frac{1}{1+m} \int_{S_2}^{\infty} P(y)\, dy \right] \delta(z - S_2) & z \geq S_2 \end{cases} \tag{18}$$

Since $P(z)$ is an even function of z it will not be necessary to define it for negative values of z. Figures 37, 38, and 39 show the curves of $P_U(z)$, $P_L(z)$, and $P(z)$ assuming

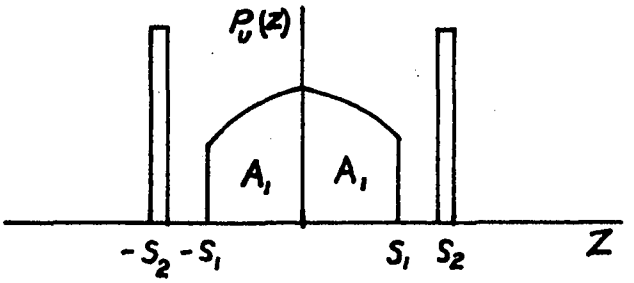

Figure 37. $P_u(Z)$ versus Z

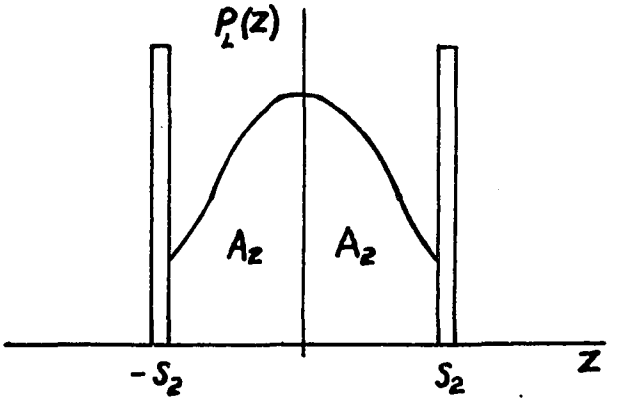

Figure 38. $P_L(Z)$ versus Z

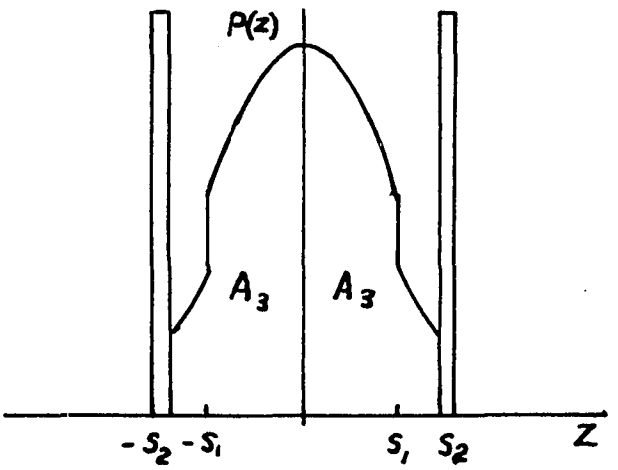

Figure 39. P(Z) versus Z

$$P(y) = \frac{1}{\sigma\sqrt{2\pi}} \, e^{-\frac{y^2}{2\sigma^2}} \tag{19}$$

B. Calculation of the Equivalent Gain of the Nonlinear Element

The equivalent gain of a nonlinear element, K_{eq}, will be defined as the ratio of the root-mean-square value of the output to the root-mean-square value of the input when the input probability density distribution is Gaussian. K_{eq} is a "statistical describing function" and is a function of σ, the root-mean-square value of the input.

1. Calculation of σ_z for the compensated system

$$\sigma_z^2 = 2 \int_0^\infty z^2 P(z) \, dz$$

$$\frac{\sigma_z^2}{2} = \frac{1}{\sigma\sqrt{2\pi}} \left[\int_0^{S_1} z^2 e^{-\frac{z^2}{2\sigma^2}} \, dz + \frac{1}{1+m} \int_{S_1}^{S_2} z^2 e^{-\frac{z^2}{2\sigma^2}} \, dz \right.$$

$$\left. + \frac{S_2^2}{1+m} \left(m \int_{S_1}^\infty e^{-\frac{y^2}{2\sigma^2}} \, dy + \int_{S_2}^\infty e^{-\frac{y^2}{2\sigma^2}} \, dy \right) \right] \tag{20a}$$

Equation 20 can be written in the form

$$\frac{\sigma_z^2}{2} = \frac{1}{\sigma\sqrt{2\pi}}\left[\int_0^{S_1} z^2 e^{-\frac{z^2}{2\sigma^2}} dz + \frac{1}{1+m}\left(\int_0^{S_2} z^2 e^{-\frac{z^2}{2\sigma^2}} dz - \right.\right. \tag{20b}$$

$$\left.\left.\int_0^{S_1} z^2 e^{-\frac{z^2}{2\sigma^2}} dz\right) + \frac{S_2^2}{1+m}\left(m\int_{S_1}^{\infty} e^{-\frac{y^2}{2\sigma^2}} dy + \int_{S_2}^{\infty} e^{-\frac{y^2}{2\sigma^2}} dy\right)\right]$$

Collecting terms we have

$$\frac{\sigma_z^2}{2} = \frac{1}{(1+m)\sigma\sqrt{2\pi}}\left[m\int_0^{S_1} z^2 e^{-\frac{z^2}{2\sigma^2}} dz + \int_0^{S_2} z^2 e^{-\frac{z^2}{2\sigma^2}} dz\right.$$

$$\left. + S_2^2\left(m\int_{S_1}^{\infty} e^{-\frac{y^2}{2\sigma^2}} dy + \int_{S_2}^{\infty} e^{-\frac{y^2}{2\sigma^2}} dy\right)\right] \tag{21}$$

It can be shown by integration by parts that

$$\int_0^{S_a} z^2 e^{-\frac{z^2}{2\sigma^2}} dz = \sigma^2\left(-S_a e^{-\frac{S_a^2}{2\sigma^2}} + \int_0^{S_a} e^{-\frac{z^2}{2\sigma^2}} dz\right) \tag{22}$$

$$\frac{1}{2}\left(\frac{\nabla z}{\nabla}\right)^2 = \frac{m}{1+m}\left(-\frac{1}{\sqrt{2\pi}}\,\frac{S_1}{\nabla}\,e^{-\frac{1}{2}\left(\frac{S_1}{\nabla}\right)^2} + \frac{1}{\sqrt{2\pi}}\int_0^{\frac{S_1}{\nabla}} e^{-\frac{1}{2}\left(\frac{z}{\nabla}\right)^2} d\left(\frac{z}{\nabla}\right)\right)$$

$$+\frac{1}{1+m}\left(-\frac{1}{\sqrt{2\pi}}\,\frac{S_2}{\nabla}\,e^{-\frac{1}{2}\left(\frac{S_2}{\nabla}\right)^2} + \frac{1}{\sqrt{2\pi}}\int_0^{\frac{S_2}{\nabla}} e^{-\frac{1}{2}\left(\frac{z}{\nabla}\right)^2} d\left(\frac{z}{\nabla}\right)\right)$$

$$+\frac{m}{1+m}\left(\left(\frac{S_2}{\nabla}\right)^2\frac{1}{\sqrt{2\pi}}\int_{\frac{S_1}{\nabla}}^{\infty} e^{-\frac{1}{2}\left(\frac{y}{\nabla}\right)^2} d\left(\frac{y}{\nabla}\right)\right)$$

$$+\frac{1}{1+m}\left(\left(\frac{S_2}{\nabla}\right)^2\frac{1}{\sqrt{2\pi}}\int_{\frac{S_2}{\nabla}}^{\infty} e^{-\frac{1}{2}\left(\frac{y}{\nabla}\right)^2} d\left(\frac{y}{\nabla}\right)\right) \qquad (23)$$

For the sake of brevity Equation 23 will be written in the following form:

$$\frac{1}{2}\left(\frac{\nabla_z}{\nabla}\right)^2 = T\left[-\frac{S_1}{\nabla}U + W\right] + R\left[-\frac{S_2}{\nabla}V + Y\right] + TX + RZ \qquad (24)$$

where R, T, U, V, W, X, Y and Z are defined by Equations 23 and 24.

2. Calculation of ∇z for the uncompensated system

$$P(z) = \begin{cases} \frac{1}{\nabla\sqrt{2\pi}}\, e^{-\frac{z^2}{2\nabla^2}} & 0 < z < S_2 \\ \left(\frac{1}{\nabla\sqrt{2\pi}}\int_{S_2}^{\infty} e^{-\frac{y^2}{2\nabla^2}}\, dy\right) + \delta(S - S_2) & z \geq S_2 \end{cases} \qquad (25)$$

and

$$\frac{1}{2}\sigma_z^2 = \frac{1}{\sigma\sqrt{2\pi}}\int_0^{S_2} z^2 e^{-\frac{z^2}{2\sigma^2}} dz + S_2^2\left(1 - \frac{1}{\sigma\sqrt{2\pi}}\int_{-\infty}^{S_2} e^{-\frac{y^2}{2\sigma^2}} dy\right)$$

$$\frac{1}{2}\sigma_z^2 = \sigma^2\left[-\frac{S_2}{\sigma\sqrt{2\pi}} e^{-\frac{1}{2}\left(\frac{S_2}{\sigma}\right)^2} + \frac{1}{\sqrt{2\pi}}\int_0^{\frac{S_2}{\sigma}} e^{-\frac{1}{2}\left(\frac{z}{\sigma}\right)^2} d\left(\frac{z}{\sigma}\right)\right.$$

$$\left. + \frac{S_2^2}{\sigma^2}\left(1 - \frac{1}{\sqrt{2\pi}}\int_{-\infty}^{\frac{S_2}{\sigma}} e^{-\frac{1}{2}\left(\frac{y}{\sigma}\right)^2} d\left(\frac{y}{\sigma}\right)\right)\right] \qquad (26)$$

Thus we can obtain

$$\frac{1}{2}\left(\frac{\sigma_z}{\sigma}\right)^2 = -\frac{1}{\sqrt{2\pi}}\frac{S_2}{\sigma} e^{-\frac{1}{2}\left(\frac{S_2}{\sigma}\right)^2} + \frac{1}{\sqrt{2\pi}}\int_0^{\frac{S_2}{\sigma}} e^{-\frac{1}{2}\left(\frac{z}{\sigma}\right)^2} d\left(\frac{z}{\sigma}\right)$$

$$+ \left(\frac{S_2}{\sigma}\right)^2\left(1 - \frac{1}{\sqrt{2\pi}}\int_{-\infty}^{\frac{S_2}{\sigma}} e^{-\frac{1}{2}\left(\frac{y}{\sigma}\right)^2} d\left(\frac{y}{\sigma}\right)\right) \qquad (27)$$

Again for brevity we write

$$\frac{1}{2}\left(\frac{\sigma_z}{\sigma}\right)^2 = A + B + C \qquad (28)$$

where Equations 27 and 28 define A, B and C. The calculation of K_{eq} for both the compensated and uncompensated systems is now straightforward, but

tedious, and is shown in tabulated form in Tables 13 through 19 with a summary of the results shown in Table 20.

3. Results

The results of the calculations of the statistical describing functions, K_{eq}, are plotted in Figure 39 for the compensated and uncompensated systems as a function of $\sqrt{\ }$. For the curves plotted, the dropout point of the hysteresis compensator, S_1, was set at 0.12 units and the saturation level of the limiter was 0.5 units.

The output amplitude probability density distribution of a nonlinear element that is subject to a Gaussian input is not Gaussian. It has been shown by a number of authors, among them, Chaung and Kazda (15) and Rice (16) that the average feedback control system behaves like a low-pass filter and has a tendency to redistribute the signals in such a way as to produce a Gaussian form. This idea leads to the assumption that the output of a nonlinear element in a feedback control system, when fed back through frequency sensitive elements and combined with a Gaussian input signal, produces a Gaussian error signal. It is necessary that the above assumption be made in order to proceed with the analysis of the error response of a nonlinear system when subjected to a Gaussian input.

C. Equivalent Gain Error Response

Thaler and Pastel (11) outline an approximate method for calculating the system response of a nonlinear control system subjected to a random input. It consists of replacing the nonlinear element by a linear element whose gain is K_{eq} (the statistical describing function). K_{eq} is a function of the root-mean-square value of the signal at the input of the non-

Table 13. Calculation of σ_z for the compensated system

σ	$S_{1/\sigma}$	$S_{2/\sigma}$	W	σ^2 X	Y	σ^2 Z
0						
.25	.48	2.0	0.1844	0.3156	0.4772	.0228
.50	.24	1.0	0.0948	0.4052	0.3413	.1587
.75	.16	.67	0.0636	0.4364	0.2486	.2514
1.00	.12	.50	0.0478	0.4522	0.1915	.3058
1.25	.096	.40	0.0382	0.4579	0.1554	.3446
1.50	.080	.333	0.0319	0.4867	0.1305	.4695

Table 14. Calculation of ∇z for the compensated system

τ	m	R	T	S_1/τ	U	$-S_1 U/\tau$	W	$\left(\frac{-S_1}{\tau} U + W\right)$	$T\left[\frac{S_1}{\tau} U + W\right]$
0									
.25	0.0334	0.986	0.032	.48	.3555	-0.17	0.1844	0.0144	.00046
.50	0.267	0.790	0.210	.24	.3876	-0.093	0.0948	0.0018	.000378
.75	0.447	0.692	0.308	.16	.3939	-0.063	0.0636	0.0003	.000093
1.00	0.564	0.640	0.360	.12	.3961	-0.0475	0.0478	0.0003	.000108
1.25	0.640	0.610	0.388	.096	.3970	-0.6382	0.0382	0	0
1.50	0.881	0.532	0.468	.080	.3977	-0.0320	0.0319	0	0

Table 15. Calculation of τ_z for the compensated system

τ	m =	R	$\frac{S_2}{\tau}$	V	$-\frac{S_2}{\tau} V$	Y	$(-\frac{S_2}{\tau} V + Y)$	$R(-^{S_2}V + Y)$
0								
.25	0.0334	0.968	2.00	0.0540	-0.1080	0.4772	0.3692	0.3580
.50	0.267	0.790	1.00	0.2420	-0.2420	0.3413	0.0993	0.0784
.75	0.447	0.692	0.67	0.3187	-0.2137	0.2486	0.0347	0.0240
1.00	0.564	0.640	0.50	0.3521	-0.1760	0.1915	0.0155	0.0099
1.25	0.640	0.610	0.40	0.3683	-0.1475	0.1554	0.0079	0.0051
1.50	0.881	0.532	0.333	0.3773	-0.1255	0.1305	0.0050	0.0026

Table 16. Calculation of ∇z for the compensated system

∇	T	$(S_2)^2$	X	$T(S_2)^2 X$	R	$(S_2)^2$	Z	$R(S_2)^2 Z$
0								
.25	0.032	.25	0.3156	0.040	0.968	.25	0.0228	0.0880
.50	0.210	.25	0.4052	0.0852	0.790	.25	0.1587	0.1250
.75	0.308	.25	0.4364	0.0597	0.692	.25	0.2514	0.0775
1.00	0.360	.25	0.4522	0.0411	0.640	.25	0.3085	0.0494
1.25	0.388	.25	0.4579	0.0285	0.610	.25	0.3446	0.0336
1.50	0.468	.25	0.4867	0.0253	0.532	.25	0.4695	0.0278

Table 17. Calculation of τ_z for the compensated system

τ	$T[-\frac{S_1}{\tau} U + W]$	$R[-\frac{S_2}{\tau} V + Y]$	$T(S_2)^2$ X	$R(S_2)^2$ Z	$\frac{1}{2}\left(\frac{\tau_z}{\tau_y}\right)^2$	$\frac{(\tau_z)^2}{(\tau_y)^2}$	$\frac{\tau_z}{\tau_y} = K_{eq}$
0						1.000	1.000
.25	0.00046	0.358--	0.0404-	0.0880-	0.48686	0.97362	0.987
.50	0.000378	0.078400	0.0852--	0.1250--	0.288978	0.577956	0.760
.75	0.000093	0.024---	0.0597--	0.0775	0.161293	0.322586	0.568
1.00	0.000108	0.0099--	0.0411--	0.0494--	0.100508	0.201016	0.450
1.25	0	0.00510	0.0285-	0.0336-	.06720	0.13440	0.367
1.50	0	0.0026	0.0253	0.0278	.0557	0.1114	0.334

Table 18. Calculation of K_{eq} for uncompensated system

Γ	S_2/Γ	A	B	C
.25	2.0	- .1080	.4772	.0912
.50	1.0	- .2420	.3413	.1587
.75	.67	- .2135	.2486	.1120
1.00	.50	- .1761	.1915	.0772
1.25	.40	- .1473	.1559	.0550
1.50	.333	- .1257	.1300	.0411

Table 19. Calculation of K_{eq} for uncompensated system

	$\frac{1}{2}\frac{(\tau_z)^2}{(\tau_y)^2}$	$\left(\frac{\tau_z}{\tau_y}\right)^2$	$\tau_{z/\tau y} = K_{eq}$
.25	.4604	.9208	0.96
.50	.2580	.5160	0.72
.75	.1371	.2742	0.523
1.00	.0926	.1852	0.430
1.25	.06311	.1262	0.356
1.50	.6454	.0908	0.301

Table 20. Comparison of K_{eq} for compensated and uncompensated systems

$S_1 = 0.12 \quad S_2 = 0.5$

γ	K_{eq} Uncompensated	K_{eq} Compensated
0	1.00	1.00
0.25	0.960	0.987
0.50	0.720	0.760
0.75	0.523	0.568
1.00	0.430	0.450
1.25	0.356	0.367
1.50	0.301	0.334

linear element and is plotted versus σ in Figure 40a.

The system to be analyzed is shown in Figure 41. From the diagram it can be seen that the error signal which is also the input to the nonlinear element is

$$E(s) = \frac{R(s)}{1 + G(s)\ H(s)} = \frac{s(s + 2\zeta)\ R(s)}{s^2 + 2\ \zeta s + K_{eq}} \qquad (29)$$

It will be assumed that the system is subject to a random input with Gaussian distribution and a power frequency spectrum given by

$$\phi_R(\omega) = \frac{1}{1 + j\omega} \cdot \frac{1}{1 - j\omega} \qquad (30)$$

The power frequency spectrum of the error signal is

$$\phi_E(\omega) = \frac{[(j\omega)^2 + 2\zeta j\omega][(-j\omega)^2 - 2\zeta j\omega]}{[(j\omega)^2 + 2\zeta j\omega + K_{eq}][1 + j\omega][(-j\omega)^2 - 2\zeta j\omega + K_{eq}][1 - j\omega]}$$

or

$$\phi_E(\omega) = \frac{\omega^4 + 4\ \zeta^2\ \omega^2}{[-j\omega^3 - (1+2\zeta)\omega^2 + j(K_{eq} + 2\zeta)\omega + K_{eq}][\ \text{Conjugate}\ ]} \qquad (31)$$

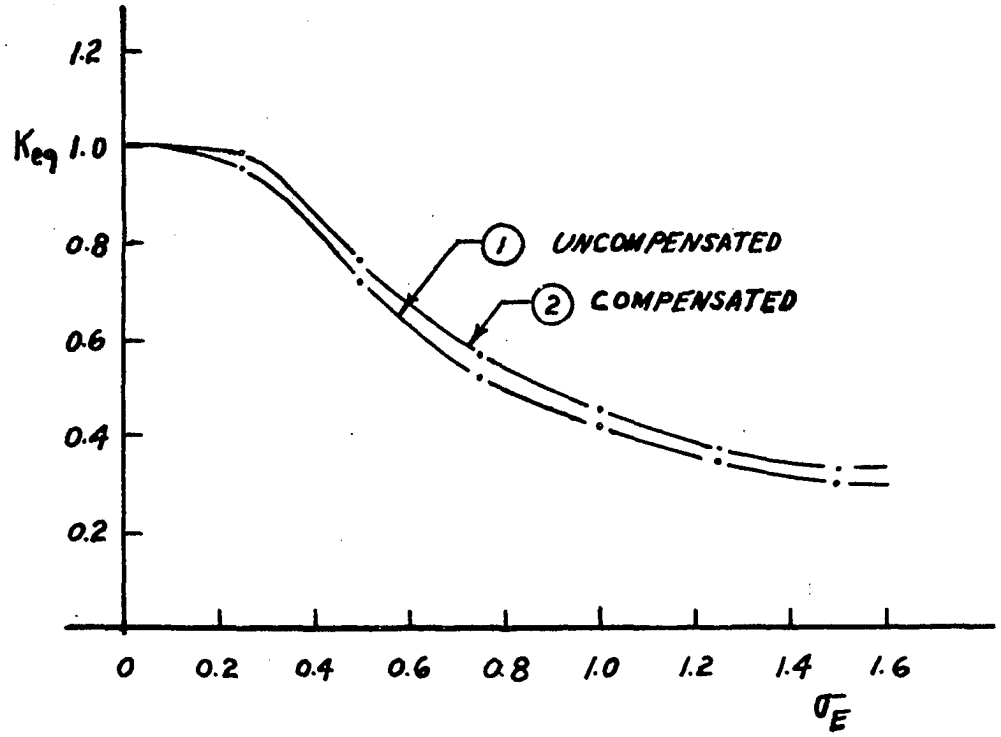

Figure 40a. K_{eq} versus σ_E for compensated and uncompensated systems

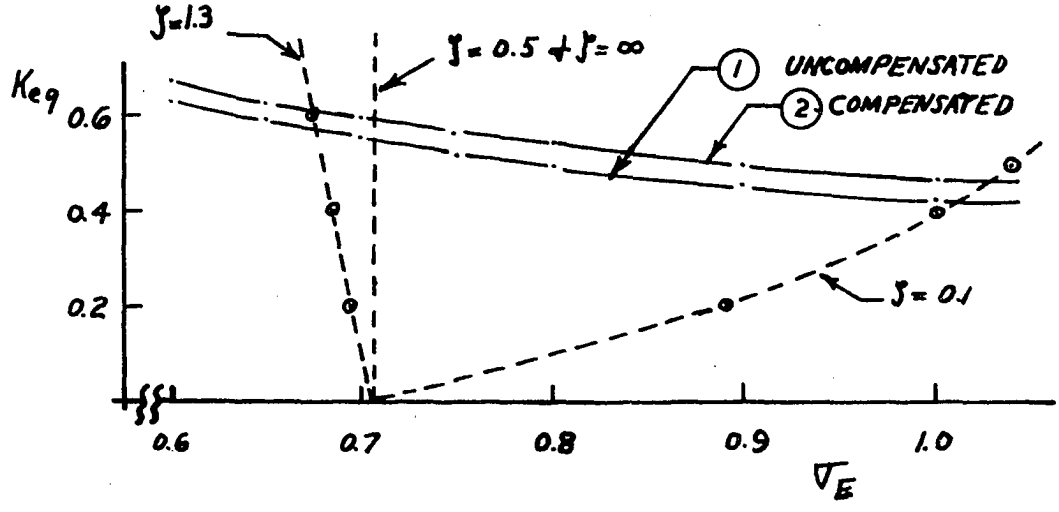

Figure 40b. Curves of K_{eq} calculated from Equation 35 superimposed on expanded portion of Figure 40a

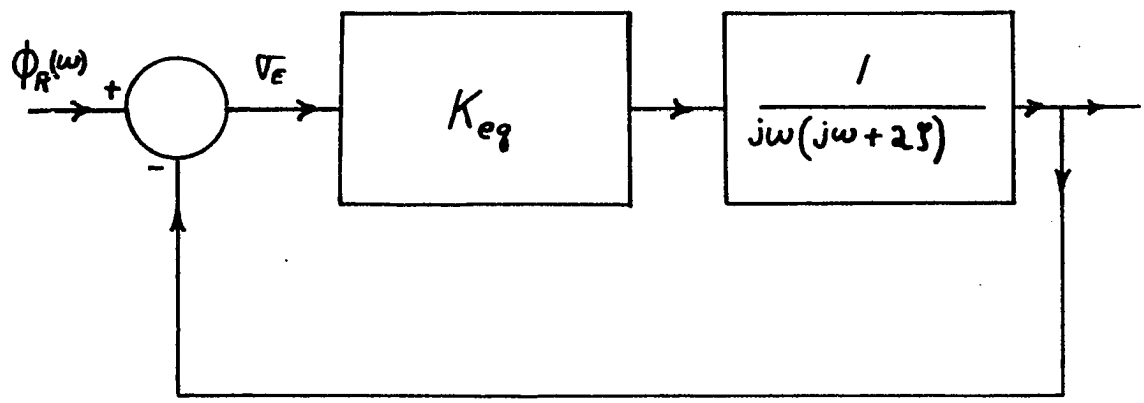

Figure 41. Second order system with random input

Thus the mean-square value of the error signal is

$$\sigma_E^2 = \frac{1}{2\pi j} \int_{-\infty}^{\infty} \frac{j\omega^4 + j4\zeta^2\omega^2}{[-j\omega^3 - (1+2\zeta)\omega^2 + j(K_{eq} + 2\zeta)\omega + K_{eq}][\text{ Conjugate }]} d\omega \tag{32}$$

This integral is of the form discussed by Brown and Nilsson (17)

$$I_n = \int_{-\infty}^{\infty} \frac{g_n(x)}{h_n(x)\ h_n(-x)} dx$$

where

$$h_n(x) = a_o x^n + a_1 x^{n-1} + \ldots + a_n$$

$$g_n(x) = b_o x^{2n-2} + b_1 x^{2n-4} + \ldots + b_{n-1}$$

here

$$a_o = -j \qquad b_o = j$$

$$a_1 = -(1 + 2\zeta) \qquad b_1 = j4\zeta^2$$

$$a_2 = j(K_{eq} + 2\zeta) \qquad b_2 = 0$$

$$a_3 = K_{eq} \tag{33}$$

The value of the integral is given as

$$I_3 = \frac{-a_2 b_o + a_o b_1 - \frac{a_o a_1 b_2}{a_3}}{2a_o (a_o a_3 - a_1 a_2)} \tag{34}$$

After substitution and simplification the integral is evaluated as

$$\sigma_E^2 = I_3 = \frac{K_{eq} + 2\zeta(1 + 2\zeta)}{4\zeta(1 + 2\zeta + K_{eq})} \tag{35}$$

From Equation 35 the gain, K_{eq}, can be expressed as a function of the root-mean-square value of the input to the nonlinear element which is also the system error.

Figure 40a and Equation 35 give two relationships to be satisfied by K_{eq} simultaneously for the given input signal. Analytic solution of the two equations is not feasible but a simultaneous solution can be obtained graphically by plotting curves of K_{eq} versus σ for Equation 35 on the same sheet of paper with the curve of Figure 40a. The intersection of the two curves gives the root-mean-square error of the system.

In Figure 40b an expanded portion of the curves of Figure 40a are plotted along with curves calculated from Equation 35 for damping ratios of 0.1, 0.5, 1.3 and infinity. Table 21 gives the calculated results used for plotting the curves. The curves for a damping ratio of 0.5 and infinity are vertical lines at $\sigma = 0.707$. The curves for all damping ratios between 0.5 and infinity lie between the vertical line at $\sigma = 0.707$ and the curve for a damping ratio of 1.3 and have a negative slope. Curves for all

Table 21. ∇_E calculated from Equation 35

K_{eq}	1.0	0.8	0.6	0.4	0.2	0
$\zeta = 0.1$	1.19	1.14	1.08	1.00	0.89	0.707
$\zeta = 0.5$	0.707	0.707	0.707	0.707	0.707	0.707
$\zeta = 1.0$	0.662	0.670	0.677	0.686	0.695	0.707
$\zeta = 1.3$	0.660	0.666	0.674	0.685	0.695	0.707
$\zeta = \infty$	0.707	0.707	0.707	0.707	0.707	0.707

damping ratios less than 0.5 lie to the right of the $\sigma_E = 0.707$ line and have a positive slope.

The curves of Figure 40b predict that for a random input to the system an increase in the equivalent gain would reduce the root-mean-square value of the error signal for the system studied if the damping ratio is between 0.5 and infinity, with the maximum reduction occurring for a damping ratio in the vicinity of 1.0. The value of damping ratio at which the maximum reduction occurs is a function of K_{eq} at the point of intersection of the curves. It can be found by taking the derivative of $(\sigma_E)^2$ with respect to the damping ratio, setting the result equal to zero and solving for the damping ratio.

The calculations are as follows:

$$\frac{d(\sigma_E)^2}{d\zeta} = \frac{d}{d\zeta}\left[\frac{K_{eq} + 2\zeta + 4\zeta^2}{8\zeta^2 + 4\zeta(K_{eq} + 1)}\right]$$

$$\frac{d(\sigma_E)^2}{d\zeta} = \frac{8\zeta^2 + (4K_{eq} + 4)\zeta][8\zeta + 2] - [K_{eq} + 2\zeta + 4\zeta^2][16\zeta + 4K_{eq} + 4]}{[8\zeta^2 + 4\zeta(K_{eq} + 1)]^2} \qquad (36)$$

Setting the numerator equal to zero and solving for ζ we can obtain

$$\zeta = 0.5 \pm 0.5\sqrt{2 + K_{eq}} \qquad (37)$$

The possibility of a negative value for ζ will not be considered due to the nature of the problem and thus the value of ζ which will give a minimum

value of root-mean-square error is

$$\zeta_{(\text{min.error})} = 0.5 + 0.5\sqrt{2 + K_{eq}} \qquad (38)$$

If a value of $K_{eq} = 0.6$ (the approximate value of K_{eq} at the operating point of the system) is substituted into Equation 38, the value of damping ratio which will give a minimum error is approximately 1.3.

For values of damping ratio smaller than 0.5 Figure 40b predicts that an increase in equivalent gain such as produced by a hysteresis compensator would have a tendency to increase the root-mean-square error for a random input.

The preceding results do not show a significant change in error produced by the hysteresis compensator. It would appear from the above analysis that the hysteresis-compensated system with a damping ratio larger than 0.5 would be only very slightly more susceptible to a random noise signal at the input than would the uncompensated system. An interesting observation is that the range of values of damping ratio for which the hysteresis compensator is capable of reducing the root-mean-square error for a random input is precisely the range of values for which it has been found to be effective in improving the step response.

VI. SUMMARY

In the preceding sections the use of the hysteresis element to compensate for saturation in a position-control servomechanism has been studied for the purpose of:

1. Determining the conditions under which such a compensator can be effective.
2. Arriving at an orderly design procedure which allows one to quickly design a hysteresis compensator that will be effective.

The effectiveness of the hysteresis compensator was found to depend chiefly on two factors, the damping ratio of the system, and the magnitude of the input steps relative to the saturation level of the system. The hysteresis compensator was found to be effective for systems with damping ratios larger than 0.5, becoming more effective as the damping of the system is increased. For critically damped and overdamped systems, it was found possible to design the hysteresis compensator in such a way as to give a step response very close to the time-optimal response for the system. The hysteresis compensator was not found to be effective in improving the step-input performance of systems with damping ratios smaller than 0.5.

The amount of improvement possible in the settling time of a heavily damped system was found to be practically a constant value for inputs large enough that the system became velocity-limited before the dropout point was reached. This means that the percentage improvement in time of response decreases as the input steps are increased to large values.

In Section IV the method of design was extended to apply to a third-order system through the use of an analog computer. The design pro-

cedure and results were found to be essentially the same for the third-order system as they were for the second-order system.

Finally, an estimate of the response of a hysteresis-compensated system to a random input was obtained in Section V. The results of this analysis indicate that the use of a hysteresis element would have little, if any, effect on the susceptibility of the system to random noise.

In concluding, it can be said that the hysteresis compensator, like most nonlinear compensators, has definite limitations on its usefulness. It can be useful to improve the step response for a system made sluggish by inherent saturation or it can be used to achieve improved performance of control systems with less cost by operating the elements at their maximum capabilities which almost always implies saturation of some element of the system. Although the hysteresis compensator is a form of nonlinear compensator designed primarily to improve step-input performance, it does not, like some nonlinear compensators,have a detrimental effect when the input is something other than a step input.

VII. LITERATURE CITED

1. West, John C. Analytical techniques for nonlinear control systems. D. Van Nostrand Company, Inc. Princeton, New Jersey. 1960.

2. Hopkin, A. M. Compensation of saturating servos. American Institute of Electrical Engineers Transactions 70: 631-639. 1951.

3. Chen, Kan. Quasi-linearization design of nonlinear feedback control systems. Unpublished paper presented at Joint Automatic Control Conference, Minneapolis, Minnesota, June, 1963. Mimeographed. New York, New York, American Institute of Chemical Engineers. 1963.

4. Chang, S. S. L. and Archibald, R. W. Compensating saturation in feedback control systems by excess error storage. American Institute of Electrical Engineers Transactions 77: 16-20. 1958.

5. Kalman, R. E. Analysis and design principles of second and higher order saturating servomechanisms. American Institute of Electrical Engineers Transactions 74: 294-310. 1955.

6. Golden, W. H. and Weaver, C. H. A study of contactor servomechanisms with positive hysteresis. Institute of Electrical and Electronic Engineers Transactions on Applications and Industry 66: 105-111. 1963.

7. Pell, W. H. Graphical solution of single-degree-of-freedom vibration problem with arbitrary damping and restoring forces. Journal of Applied Mechanics 24: 311-312. 1957

8. Bellman, R. Dynamic programming. Princeton University Press. Princeton, New Jersey.

9. Pontryagin, L. S., Boltyanski, V. G., Gamrelidze, R. V., and Mischenko, E. F. Mathematical theory of optimal processes. Interscience Publishers, Inc. New York.

10. Gibson, John E. Nonlinear automatic control. McGraw-Hill Book Company, Inc. New York. 1963.

11. Thaler, George J. and Pastel, Marvin P. Analysis and design of nonlinear feedback control systems. McGraw-Hill Book Company, Inc. 1962.

12. Cosgrift, Robert Lien, Nonlinear control systems. McGraw-Hill Book Company, Inc. New York. 1958.

13. Truxal, J. G. Automatic feedback control system synthesis. McGraw-Hill Book Company, Inc. New York. 1955.

14. Bogner, I. and Kazda, L. F. Switching criteria for higher order servos. American Institute of Electrical Engineers Transactions 73: 118-127. 1954.

15. Chaung, Kuei and Kazda, L. F. A study of nonlinear systems with random inputs. American Institute of Electrical Engineers Transactions 78: 100-106. 1959.

16. Rice, S. O. Mathematical analysis of random noise. Bell System Technical Journal 23: 282. 1944.

17. Brown, Robert Grover and Nilsson, James William. Introduction to linear systems analysis. John Wiley and Sons, Inc. New York. 1962

VIII. ACKNOWLEDGEMENTS

The author wishes to gratefully acknowledge the guidance and assistance of his major professor, Dr. R. Grover Brown. Thanks are due also to Distinguished Professor W. L. Cassell who served as chairman of the original committee and to Dr. James W. Nilsson for his guidance and encouragement during the early part of the study.